

2

NAVAL POSTGRADUATE SCHOOL

Monterey, California

AD-A225 917

DTIC
LECTE
JG 2 0 1990

D

D



DTIC FILE COPY

THESIS

NUCLEATE POOL BOILING PERFORMANCE OF
FINNED AND HIGH FLUX
TUBE BUNDLES IN R-114/OIL MIXTURES

by

Nezih Akcasayar

December 1989

Thesis Advisor

Paul J. Marto

Approved for public release; distribution is unlimited.

Unclassified

security classification of this page

REPORT DOCUMENTATION PAGE				
1a Report Security Classification Unclassified			1b Restrictive Markings	
2a Security Classification Authority			3 Distribution Availability of Report	
2b Declassification Downgrading Schedule			Approved for public release; distribution is unlimited.	
4 Performing Organization Report Number(s)			5 Monitoring Organization Report Number(s)	
6a Name of Performing Organization Naval Postgraduate School		6b Office Symbol (if applicable) 570	7a Name of Monitoring Organization Naval Postgraduate School	
6c Address (city, state, and ZIP code) Monterey, CA 93943-5000			7b Address (city, state, and ZIP code) Monterey, CA 93943-5000	
8a Name of Funding Sponsoring Organization		8b Office Symbol (if applicable)	9 Procurement Instrument Identification Number	
8c Address (city, state, and ZIP code)			10 Source of Funding Numbers	
			Program Element No	Project No
			Task No	Work Unit Accession No
11 Title (include security classification) NUCLEATE POOL BOILING PERFORMANCE OF FINNED AND HIGH FLUX TUBE BUNDLES IN R-114 OIL MIXTURES				
12 Personal Author(s) Neziñ Akcasayar				
13a Type of Report Master's Thesis		13b Time Covered From To		15 Page Count 91
14 Date of Report (year, month, day) December 1989				
16 Supplementary Notation The views expressed in this thesis are those of the author and do not reflect the official policy or position of the Department of Defense or the U.S. Government.				
17 Cosati Codes			18 Subject Terms (continue on reverse if necessary and identify by block number)	
Field	Group	Subgroup	Heat Transfer, Pool boiling.	
19 Abstract (continue on reverse if necessary and identify by block number)				
<p>The heat transfer characteristics of pure R-114 and R-114:oil mixtures during nucleate pool boiling from a small bundle of finned and High Flux tubes were measured. The bundles had 5 instrumented and 10 additional heated tubes of 15.8 mm outside diameter which were arranged in an equilateral triangular pitch of 19.1 mm giving a pitch-to-diameter ratio of 1.2. Pure refrigerant with York-C lubrication oil mass concentrations of 1, 2, 3, 5 and 10% was used. All experiments were performed at 2.2 C corresponding to a pressure slightly below atmospheric.</p> <p>Data sets were taken using decreasing heat flux only in order to avoid the boiling hysteresis phenomenon. An enhancement in heat-transfer performance of the finned tube bundle due to oil applications was observed. The enhancement increased with up to 3% oil concentration over all heat flux ranges. Further oil additions showed better performances than pure R-114 at high heat flux levels but poorer performance was obtained at lower heat fluxes. High Flux tube experiments indicated that the heat transfer performance of the bundle was approximately 2.5 times better than the finned tube bundle performance for pure R-114. No positive performance enhancement was observed from the High Flux tube bundle due to oil addition. The performance immediately degraded with 1% oil and stayed almost constant with 2% and 3% oil additions. A decrease of performance became significant at high heat flux levels with oil concentrations of 6% and 10%.</p> <p>The performance of these two tube bundles was compared to smooth tube operation.</p>				
20 Distribution Availability of Abstract			21 Abstract Security Classification	
<input checked="" type="checkbox"/> unclassified unlimited <input type="checkbox"/> same as report <input type="checkbox"/> DTIC users			Unclassified	
22a Name of Responsible Individual Paul J. Marto			22b Telephone (include Area code) (408) 646-2768	22c Office Symbol 54Ss

DD FORM 1473,84 MAR

83 APR edition may be used until exhausted
All other editions are obsolete

security classification of this page

Unclassified

Approved for public release; distribution is unlimited.

Nucleate Pool Boiling Performance Of Finned And High Flux
Tube Bundles In R-114/Oil Mixtures

by

Nezih Akcasayar
Lieutenant Junior Grade, Turkish Navy
B.S., Turkish Naval Academy, 1983

Submitted in partial fulfillment of the
requirements for the degree of

MASTER OF SCIENCE IN MECHANICAL ENGINEERING

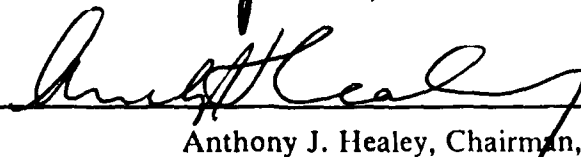
from the

NAVAL POSTGRADUATE SCHOOL
December 1989

Author:


Nezih Akcasayar

Approved by:


Paul J. Marto, Thesis Advisor
Anthony J. Healey, Chairman,
Department of Mechanical Engineering

ABSTRACT

The heat transfer characteristics of pure R-114 and R-114/oil mixtures during nucleate pool boiling from a small bundle of finned and High Flux tubes were measured. The bundles had 5 instrumented and 10 additional heated tubes of 15.8 mm outside diameter which were arranged in an equilateral triangular pitch of 19.1 mm giving a pitch-to-diameter ratio of 1.2. Pure refrigerant with York-C lubrication oil mass concentrations of 1, 2, 3, 6 and 10% was used. All experiments were performed at 2.2C corresponding to a pressure slightly below atmospheric.

Data sets were taken using decreasing heat flux only in order to avoid the boiling hysteresis phenomenon. An enhancement in heat-transfer performance of the finned tube bundle due to oil applications was observed. The enhancement increased with up to 3% oil concentration over all heat flux ranges. Further oil additions showed better performances than pure R-114 at high heat flux levels but poorer performance was obtained at lower heat fluxes. High flux tube experiments indicated that the heat transfer performance of the bundle was approximately 2.5 times better than the finned tube bundle performance for pure R-114. No positive performance enhancement was observed from the High Flux tube bundle due to oil addition. The performance immediately degraded with 1% oil and stayed almost constant with 2% and 3% oil additions. A decrease of performance became significant at high heat flux levels with oil concentrations of 6% and 10%.

The performance of these two tube bundles was compared to smooth tube operation.

TABLE OF CONTENTS

I. INTRODUCTION	1
A. BACKGROUND	1
B. OBJECTIVES	1
II. LITERATURE SURVEY	3
A. THEORETICAL STUDIES	3
B. EXPERIMENTAL STUDIES	4
III. EXPERIMENTAL APPARATUS	7
A. TEST APPARATUS OVERVIEW	7
B. DATA ACQUISITION SYSTEM/INSTRUMENTATION	9
C. AUXILIARY EQUIPMENT	9
1. 8 Ton Refrigeration Unit:	9
2. Ethylene Glycol-Water Mixture:	9
3. Pumps:	9
4. Flowmeters:	10
D. ENHANCED SURFACE TEST TUBES	10
1. Finned Tube	10
2. High Flux tube	10
IV. EXPERIMENTAL PROCEDURES	19
A. MANUFACTURE OF INSTRUMENTED EVAPORATOR TUBES	19
B. INSTALLATION OF EVAPORATOR TUBES AND TUBE SUPPORT BLOCK	20
C. SYSTEM EVACUATION	21
D. FREON FILL	22
E. FREON REMOVAL	22
F. GENERAL OPERATION	23
G. OIL ADDITION	23
H. DATA-REDUCTION PROCEDURES	23

V. RESULTS AND DISCUSSION	25
A. GENERAL DESCRIPTIONS	25
B. R-114 BOILING FROM FINNED TUBE BUNDLE	26
C. R-114/OIL MIXTURES BOILING FROM FINNED TUBE BUNDLE ..	27
D. R-114 BOILING FROM HIGH FLUX TUBE BUNDLE	41
E. R-114/OIL MIXTURE BOILING FROM HIGH FLUX TUBE BUNDLE	41
F. PERFORMANCE COMPARISON OF THE FINNED, HIGH FLUX AND SMOOTH TUBE BUNDLES	42
VI. CONCLUSIONS AND RECOMMENDATIONS	58
A. CONCLUSIONS	58
B. RECOMMENDATIONS	59
APPENDIX A. LISTING OF DATA FILES	60
APPENDIX B. SAMPLE CALCULATIONS	62
APPENDIX C. UNCERTAINTY ANALYSIS	70
LIST OF REFERENCES	74
INITIAL DISTRIBUTION LIST	77

Accession No.	
NTIS GRA&I	<input checked="" type="checkbox"/>
DTIC TAB	<input type="checkbox"/>
Unannounced	<input type="checkbox"/>
Justification	
By	
Distribution /	
Availability Codes	
Dist	Availability Codes
A-1	



LIST OF TABLES

Table 1.	HEATERS OF KETTLE REBOILER	7
Table 2.	COMPUTER/DATA ACQUISITION ASSIGNMENT	11
Table 3.	FINNED TUBE WALL TEMPERATURE READINGS FROM 6 THERMOCOUPLES AT A HEAT FLUX OF 90 KW/M ²	26
Table 4.	HIGH FLUX TUBE WALL TEMPERATURE READINGS FROM 6 THERMOCOUPLES AT A HEAT FLUX OF 75 KW/M ²	26
Table 5.	BOILING HEAT TRANSFER COEFFICIENTS AND ENHANCE- MENT RATIOS FOR SMOOTH TUBE BUNDLE AT A HEAT FLUX OF 30 KW/M ²	44
Table 6.	BOILING HEAT TRANSFER COEFFICIENTS AND ENHANCE- MENT RATIOS FOR FINNED TUBE BUNDLE AT A HEAT FLUX OF 30 KW/M ²	44
Table 7.	BOILING HEAT TRANSFER COEFFICIENTS AND ENHANCE- MENT RATIOS FOR HIGH FLUX TUBE BUNDLE AT A HEAT FLUX OF 30 KW/M ²	44
Table 8.	DATA FILE NAMES OF THE FINNED AND HIGH FLUX TUBE RUNS	60
Table 9.	UNCERTAINTY ANALYSIS RESULTS	73

LIST OF FIGURES

Figure 1. Schematic View of the Apparatus	13
Figure 2. Evaporator/Condenser Schematic	14
Figure 3. Front View of Evaporator	15
Figure 4. Side View of Evaporator	16
Figure 5. Sectional View of Evaporator Showing Tube Bundle	17
Figure 6. Thermocouple Locations on an Instrumented Boiling Tube and Tube Section View	18
Figure 7. Photomicrograph Showing Air Gap Between Tube and Copper Insert (Magnification 200X)	24
Figure 8. Position of Instrumented Tubes in the Tube Bundle	29
Figure 9. Single Finned Tube Performance in R-114 within Finned Tube Bundle ..	30
Figure 10. Performance Variation of Tube Number One in R-114 when Influenced by Increasing Number of Heated Tubes in Finned Tube Bundle	31
Figure 11. Heat Transfer Performance Results of Finned Tube Bundle in Pure R-114	32
Figure 12. Heat Transfer Performance Results of Finned Tube Bundle with Simu- lation Heaters in Pure R-114	33
Figure 13. Performance Variation of Tube Number One with Variation of Oil Con- centrations	34
Figure 14. Performance Variation of Tube Number One with Variation of Oil Con- centrations During Finned Tube Bundle Operation	35
Figure 15. Heat Transfer Performance Results of Finned Tube Bundle with 1% Oil Concentration	36
Figure 16. Heat Transfer Performance Results of Finned Tube Bundle with 2% Oil Concentration	37
Figure 17. Heat Transfer Performance Results of Finned Tube Bundle with 3% Oil Concentration	38
Figure 18. Heat Transfer Performance Results of Finned Tube Bundle with 6% Oil Concentration	39
Figure 19. Heat Transfer Performance Results of Finned Tube Bundle with 10% Oil Concentration	40
Figure 20. Single High Flux Tube Performance in Pure R-114 within High Flux	

Tube Bundle	45
Figure 21. Performance Variation of Tube Number one in R-114 when Influenced by Increasing Number of Heated Tubes in H. Flux Tube	46
Figure 22. Heat Transfer Performance Results of High Flux Tube Bundle in Pure R-114	47
Figure 23. Heat Transfer Performance Results of High Flux Tube Bundle with Sim- ulation Heaters in Pure R-114	48
Figure 24. Performance Variation of Tube Number One with Variation of Oil Con- centration in High Flux Tube Bundle	49
Figure 25. Heat Transfer Performance Results of High Flux Tube Bundle with 1% Oil Concentration	50
Figure 26. Heat Transfer Performance Results of High Flux Tube Bundle with 2% Oil Concentration	51
Figure 27. Heat Transfer Performance Results of High Flux Tube Bundle with 3% Oil Concentration	52
Figure 28. Heat Transfer Performance Results of High Flux Tube Bundle with 6% Oil Concentration	53
Figure 29. Heat Transfer Performance Results of High Flux Tube Bundle with 10% Oil Concentration	54
Figure 30. Comparison of High Flux, Finned and Smooth Single Tube Performances in Pure R-114	55
Figure 31. Comparison of High Flux, Finned and Smooth Top Tube Performances during Bundle Operation in Pure R-114	56
Figure 32. Comparison of High Flux, Finned and Smooth Top Tube Performances during Bundle Operation with 10% Oil concentration	57

NOMENCLATURE

SYMBOL	UNITS	NAME / DESCRIPTION
Λ_{as}	V	Voltage output from current sensor
A_c	m^2	Tube-wall cross sectional area
A_s	m^2	Area of heated surface
c_p	$J/kg\ K$	Specific heat
D_i	m	Inside tube diameter
D_o	m	Outside tube diameter
D_{tc}	m	Thermocouple location diameter
g	m/s^2	Gravitational acceleration
h	$W/m^2\ K$	Heat transfer coefficient of enhanced tube surface
h_b	$W/m^2\ K$	Heat transfer coefficient of tube unheated smooth tube ends
h_t	m	Height of freon column above a heated instrumented tube
k	$W/m\ K$	Thermal conductivity of freon
k_{cu}	$W/m\ K$	Thermal conductivity of copper
L	m	Heated length of the tube
L_u	m	Unheated length of the tube
L_c	m	Corrected unheated length of the tube
Pr		Prandtl number
p	m	Perimeter of the tube outside surface
ΔP	Pa	Hydrostatic pressure difference between tube and free surface
q	W	Heat transfer rate
q''	W/m^2	Heat flux
q_f	W	Heat transfer rate from unheated smooth tube ends
T	C	Temperature

ΔT	C	$(\bar{T}_{wo} - T_{sat})$, Wall Superheat
T_{film}	C	$(\bar{T}_{wo} + T_{sat})/2$, Film temperature
T_{film_K}	K	Film thermodynamic temperature
Tld1	C	Liquid temperature reading from thermocouple 4
Tld2	C	Liquid temperature reading from thermocouple 5
T_{sat}	C	Saturation temperature
T_{satc}	C	Corrected saturation temperature due to hydrostatic pressure difference
\bar{T}_{wi}	C	Average inside wall temperature
\bar{T}_{wi-K}	K	Average inside wall thermodynamic temperature
\bar{T}_{wo}	C	Average outside wall temperature
Vas	V	Voltage output from voltage sensor
α	m^2/s	Thermal diffusivity
β	$1/K$	Thermal expansion coefficient
μ	$kg/m\ s$	Dynamic viscosity of liquid
ν	m^2/s	Kinematic viscosity of liquid
ρ	kg/m^3	Density of liquid
Φ	C	Fourier conduction term
ψ		Variable in density calculation

ACKNOWLEDGEMENTS

I wish to express my sincere appreciation to Professor Paul J. Marto of the Mechanical Engineering department, U.S Naval Postgraduate School, for his guidance, encouragement and patience which made this study a great learning experience. Additionally, I wish to thank Thomas McCord and the Machine Shop personnel of the Mechanical Engineering department for their invaluable help.

I. INTRODUCTION

A. BACKGROUND

One of the most important goals of recent heat exchanger research is to increase the efficiency and reduce the size and cost of the present systems. As described by Nishikawa and Ito [Ref. 1], heat transfer with large temperature differences should be avoided for efficient use of heat sources. A large temperature difference will increase the irreversibility by heat transfer, and give rise to the degradation of thermal energy. It also implies larger dimensions of the heat exchanger.

When dealing with refrigerant evaporators, the use of enhanced boiling surfaces can reduce the wall superheat substantially. A variety of earlier investigations have shown that tubes with enhanced surfaces give much smaller wall superheats than smooth tubes during nucleate pool boiling. This indicates that refrigerant evaporators using enhanced tubes should be smaller in size, which is a very attractive feature for naval vessels.

During operation of refrigeration plants, some amount of oil can leak into the evaporator section from compressor seals. Since the nucleate pool boiling performance of enhanced surfaces has been found to be strongly affected by liquid composition, the effects of refrigerant/oil mixtures should be examined for enhanced evaporator tubes.

Wanniarachchi et al. [Ref. 2], compared various refrigerants which are used in naval refrigeration systems. Their comparison points out that R-114 is the best refrigerant as a working fluid in naval refrigeration systems, although other alternative refrigerants may have to be used to reduce the earth's ozone problem. The heat transfer performance of enhanced tubes in R-114/Oil mixtures is not well-documented in the literature. An experimental data base must therefore be gathered for various enhanced surfaces in a tube bundle configuration. Anderson [Ref. 3], obtained data for a bundle of smooth tubes as well as for a bundle of finned tubes. However, his finned tube data were subject to large uncertainties because of large temperature variations on his test tubes. Anderson attributed this problem to a poor thermal bond in the construction of his test tubes and recommended that an alternative technique be utilized.

B. OBJECTIVES

The objectives of this thesis are as follows:

- 1.) To manufacture and instrument a new finned tube (19 fins per inch) bundle, as well as a High Flux tube bundle and to test them in various R-114/Oil mixtures.

2.) To compare the finned and High Flux tube performances with each other and with the smooth tube performance, obtained by Anderson [Ref. 3].

II. LITERATURE SURVEY

A. THEORETICAL STUDIES

A number of correlations for nucleate pool boiling from smooth surfaces have been proposed by a number of investigators. Investigations are still being made to reach more reliable predictive equations for enhanced tubes and enhanced tube bundles.

A quick historical review of this area shows that the first investigations were made for a single plain tube. Nine different correlations for a single plain tube were listed by Chongrungreong and Sauer [Ref. 4] for nucleate pool boiling of single component fluids. They also derived a predictive equation for the heat transfer coefficient in refrigerant/oil mixtures using existing experimental data.

The commonly seen application of tube bundle evaporators made necessary the investigation of tube bundle effects. A small, triangular pitch bundle was used by Fujita et al. [Ref. 5] to obtain heat transfer correlations in a bundle. Equations were derived using rows of two and three plain tube arrangements and expanded for a row of N plain tube arrangements. Refrigerant R-113 was used in all experiments. The lower tube was evaluated as a single tube and the Mikic-Rohsenow [Ref. 6] model was applied to boiling from a single tube. For the upper tube, the surface area was divided into two segments. The first segment was the area influenced by growing bubbles; the second was the area influenced by flowing bubbles. The area influenced by flowing bubbles was also subdivided into three areas: top, sides and bottom. The correlations for heat flux were produced for each area separately and the predicted total heat flux was found by adding these expressions.

Presently, there does not exist a reliable method to predict nucleate boiling in enhanced tube bundles. Chen et al. [Ref 7] used a single finned tube (as a basis) and two finned tubes (as a simplest bundle) to investigate the pool boiling heat transfer of R-11 from enhanced surfaces both theoretically and experimentally. 19 fpi and 26 fpi finned tubes with various pitches were used in the experiments.

The theory of Mikic and Rohsenow [Ref 6] for plates and single smooth tubes was developed for a single finned tube or for the lower tube of a twin tube arrangement (which was evaluated as a single tube). In the development of single tube theory, the transferred heat flux was divided into two parts: The heat flux into the area influenced by bubbles and the heat flux into the remaining surface area due to convection. The predictive heat

flux equations were developed for each area respectively in order to obtain the single finned tube correlation using the same approach as Fujita [Ref. 5] above. For an upper finned tube, the heat flux equation for bubble influenced area was the same as for a single tube. The remaining surface was divided into three sub areas: top, sides and bottom. The respective heat transfer coefficients of each sub area was obtained and the heat transfer behavior of the upper tube was predicted. The calculated results were in good agreement with the experimental results.

Although the two tube arrangement gives information about a finned tube bundle, the variation of the top tube behavior with an increased number of heated tubes in a bundle creates new problems in predicting bundle performance. Additionally there is no predictive equation for finned tubes in refrigerant/oil mixtures, as well as for single High Flux tubes or High Flux tube bundles.

B. EXPERIMENTAL STUDIES

The usage of R-114 in refrigerating systems has become more popular due to the benefits of the refrigerant. In the past, a number of different refrigerants were used as the working fluid in systems. Most of them are still being used. There has been little investigation of nucleate boiling in R-114 from enhanced surfaces. They were mostly set up on the other refrigerants.

Danilova and Dyundin [Ref. 8] investigated the heat transfer behavior of two different finned tube bundles in R-12, R-22 and their oil mixtures. These were compared to each other and also to a smooth tube bundle. They indicated that the finned tube bundle performance was better than the smooth tube bundle and a positive "bundle effect" was observed for finned tube bundles. Additionally, the oil effect was negative on the bundle in R-12 and R-22. Sauer et al. [Ref. 9] investigated the effect of oil carryover on the boiling performance of refrigerant of R-11 at one atmosphere with finned tubing (19 fins/in.). They found that at the higher oil concentrations, boiling performance deteriorated, however, an increase in oil up to 3% did not greatly reduce the heat transfer coefficient. For oil concentrations greater than 5% the heat transfer coefficients significantly reduced. They also indicated that the effect of oil on the thermal performance of the low fin tubing was not greater than for the plain tubing. Yilmaz and Palen [Ref. 10] reported on the performance of hydrocarbon reboilers using integral low-finned (19 fins/in.) tubes and compared this performance with the result for a smooth tube bundle and for a single finned tube. Their results showed that at low boiling temperature differences, the boiling heat transfer coefficient was higher for a finned tube bundle than

for a single tube. However, at high ΔT 's, the single finned tube gave higher coefficients than the finned tube bundle. At high ΔT 's, the convection effect became less dominant relative to nucleate boiling, and probable partial vapor blanketing of the finned tube surface occurred within the bundle. These effects resulted in lower heat transfer coefficients for the finned tube bundle versus a single finned tube in their experiment. They also compared the performances of the finned and smooth tube bundles and indicated that the finned tube performance was greater than the smooth tube due to higher bubble concentration and higher circulation rate caused by a higher nucleation site density. Hahne and Muller [Ref. 11] used a finned tube (19 fin/in.) bundle consisting of 6 horizontal rows of 3 tubes each to find the performance of tubes in R-11. They determined the performance of each tube in the twin tube arrangement. They then tested several single tubes in a bundle and compared their performances to twin tube performances. They found that the bottom tube performance did not change with number of heated tubes in the bundle and stayed between upper and lower performances of the twin tube arrangement. The top tube performance increased in the same situation and it was greater than the top tube performance of the twin tube arrangement when the number of heated tubes were increased in the bundle. The rising bubbles from the lower tubes caused a convective flow in the evaporator and enhanced the performance of the upper tubes.

The performance of a single High Flux tube in refrigerants and oil mixtures was investigated and the results were published by several investigators. However, there is no documented work on High Flux tube bundle performance in refrigerant/oil mixtures. Yilmaz et al. [Ref. 12] tested a number of enhanced tubes including a High Flux tube. They obtained the heat transfer performance of the tubes in p-xylene and compared them to plain tube results. They determined that The High Flux tube performance is better than other enhanced tubes (Thermoexcel-E, Gewa-T) and much better than a smooth tube. Marto and Lepere [Ref. 13] performed similar experiments using the same type of enhanced tubes in R-113 and FC-72. They also obtained the best performance from the High Flux tube over a range of heat fluxes. The performance behavior of a single High Flux tube in R-114/oil mixtures in comparison to a single smooth tube was reported by Wanniarachchi et al [Ref. 2]. The performance of the High Flux tube was 10 times larger than that for a smooth tube in pure R-114. However, this enhancement decreased with increased oil contamination. The performance was seven times greater than that for smooth tube at heat flux of 40 kW/m^2 with 10% oil. Sawyer [Ref. 14] compared the High Flux tube performance with other enhanced tubes (Gewa-T,

Thermoexcel-E and Thermoexcel-HE) in various R-114/Oil concentrations. Above a heat flux of 18 kW/m^2 , the High Flux tube showed superior performance up to 6% oil concentration. However, at very high heat fluxes, with 6% or more oil concentration, the Gewa-T tube showed the best performance in his investigation. The newest report is provided by Grant et al. [Ref. 15] and concerns the High Flux tube performance in refrigerant/oil mixtures. They utilized R-113 in their experiments with oil concentrations up to 10%. They obtained a decreasing performance with increased oil concentrations and a significant decrease with 6% or more oil addition.

III. EXPERIMENTAL APPARATUS

A. TEST APPARATUS OVERVIEW

This chapter includes only a general description about the experimental apparatus, concentrating primarily on the evaporator section. More detailed descriptions were provided by Murphy [Ref. 16] and Anderson [Ref. 3]. Figures 1 and 2 show a schematic view of the experimental apparatus and the evaporator/condenser test apparatus, respectively.

In the condenser portion of the test apparatus, there are four instrumented horizontal smooth copper tubes in the top and five auxiliary copper condenser coils in the bottom. Each of the tubes and coils can be operated separately during experimentation. Vapor coming from the evaporator rises up and is guided toward the top of the condenser by a vapor shroud. The vapor then flows downward over the condenser tubes and coils and the condensate is returned to the evaporator section by gravity.

The evaporator is a kettle reboiler type which consists of four individually-operated sets of heaters. The names of each heater and their respective power outputs are given in Table 1.

Table 1. HEATERS OF KETTLE REBOILER

HEATERS	EACH	POWER
Instrumented Heater Tubes	5	1000 Watts/each
Active Bundle Heaters	12	1000 Watts/each
Auxiliary Heaters	4	4000 Watts/each
Simulation Heaters	5	4000 Watts/each

Front and side views of the evaporator are shown in Figures 3 and 4 respectively. Electric power can be applied separately to each set of heaters by using a STACO 240 V, 23.5 KVA rheostat controller. Also, desired numbers of auxiliary, simulation and instrumented bundle heaters can be operated by using individual circuit breakers. The four auxiliary heaters can provide up to 16 KW of heat load capacity. These heaters are used primarily as additional load for condensation experiments and secondarily for decreasing heat flux experiments under constant condenser load. The five simulation heaters have 20 KW of maximum heat load capacity. They are used to simulate an ad-

ditional number of heated tubes in the bottom part of a larger bundle. They are located at the bottom of the kettle reboiler and are separated from the test tubes by a rack of dummy tubes to guide the vapor flow. The auxiliary and simulation heaters have enough power to create a large enough local heat flux to cause freon decomposition. Great care must therefore be taken during operation of these high powered heaters in order to avoid decomposition. Dupont [Ref. 17] references the critical flux value of R-114 as 130 kW/m^2 . Configurations of all the heaters in the boiler are shown in Figure 5.

The tube bundle consists of instrumented, active and dummy tube groups. The locations of each tube group, represented by their respective letters, I, A and D, are shown in Figure 5. Among these groups, only the dummy tubes are unheated. They are used to simulate normal, large horizontal tube bundles by providing similar geometry and flow pattern. The active and instrumented tubes, which are heated, are fed electrical power by the same variac, thus providing an equal amount of voltage to each tube type. Circuit breakers are used to allow for the use of any desired number of instrumented tubes individually or in connection with active tubes.

The instrumented tubes were of two types: namely, finned tubes (19 fins per inch) and High Flux tubes. The fin-tip diameter of the finned tubes along with the outside diameter of both the High Flux and dummy tubes was 15.8 mm. The tubes were cantilevered from the back plate of the tube block with a 19.1 mm equilateral triangular pitch, giving a pitch-to-diameter ratio of 1.2. Alignment of the tubes in the front was obtained by attaching a Lexan plastic plate in which holes were drilled in such a way as to match the pitch of the tube bundles.

Both the finned and High Flux tubes were assembled locally. They consisted of an outer test tube, an inner copper sleeve and a cartridge heater in the center. The outer diameter of the copper sleeve was machined down, providing a 0.005 inch clearance with the inside of the test tube. The copper sleeve was cut with 6 $1 \text{ mm} \times 1 \text{ mm}$ grooves to accommodate the wall thermocouples. The first groove was cut to a length of 1.5 inches with subsequent lengths of each groove increasing by 1 inch. In addition, each groove was located at a 60 degree circumferential angle with the previous groove. Figure 6 shows the circumferential and longitudinal position of the thermocouple grooves in addition to an overview of the finned and High Flux tube assembly. Finally, the tubes were fabricated as described in Chapter IV.

B. DATA ACQUISITION SYSTEM/INSTRUMENTATION

A Hewlett Packard HP-3497A Data Acquisition System, HP-9125 computer and HP-701 printer were used for data acquisition, data reduction and data printing respectively. Also an HP-9826 computer and HP-7470A plotter were used to obtain vital graphs. HP Basic 3.01 was used for data reduction. At the beginning of every set of runs, the HP 9125 computer had to be initialized by using three system discs. However the HP-9826 computer did not need to be initialized. As described by Anderson [Ref. 3], type-T copper-constantan thermocouple measurements (mvolts) were made on the HP-3497A with the relay multiplexer assembly equipped with thermocouple compensation. A 20 channel relay multiplexer card was used to measure the voltage output from voltage and amperage sensors. Voltage measurements were taken from separate sensors that measured the voltage going to the tube bundle, simulation and auxiliary heaters. The total amperage going through the auxiliary and simulation heaters were each measured using an American Aerospace Control (AAC) current sensor. The currents of each instrumented tube heater were measured using five identical current sensors. The voltage supplied to the other active tubes was also measured but the current of each active tube was not. (The total current for a pair of active tubes was measured.) This was felt to be sufficient since these tubes each had the same power output (1000 W) as the test tube heaters and there was no apparent reason to monitor each active tube heat flux individually.

Computer channel assignments for data acquisition and array assignments are given in Table 2.

C. AUXILIARY EQUIPMENT

1. 8 Ton Refrigeration Unit:

This unit was used to cool the ethylene glycol-water mixture to a desired working temperature (-20 C).

2. Ethylene Glycol-Water Mixture:

This mixture was used as the coolant to remove heat from the condenser during experimentation.

3. Pumps:

There were two pumps available to pump coolant from the sump through the condenser. The primary condenser tubes and one of the secondary condenser coils were fed by pump #1. Pump #2 was used to feed four secondary condenser coils. Pump #1

was sufficient while only five instrumented tubes were run, however during bundle and simulation heater operations, both pumps were needed.

4. Flowmeters:

Five calibrated float-type flowmeters, which were connected to pump #1, were used to show the flow rate passing through four primary condenser tubes and one secondary condenser coil. Also, one additional flowmeter which was connected to pump #2, was used to measure the total flow rate of the four secondary condenser coils.

D. ENHANCED SURFACE TEST TUBES

1. Finned Tube

Wieland Type K finned tubes were used in the first part of the experiment. These tubes were obtained by roll forming the outer surface of a plain tube. They were designed and produced to stand up against very high thermal and mechanical stresses. Some properties of the tube are given below:

Fin pitch = 1.35 mm

Fin height = 1.50 mm

Mean fin thickness = 0.3 mm (approximately)

Root diameter = 12.7 mm

Tube inside diameter = 10.7 mm

Fin tip diameter = 15.8 mm

2. High Flux tube

The High Flux tubes were prepared by Linde Division of Union Carbide Corporation for our experiments. This type of tube is manufactured by applying a mixture of metal and braze alloys to a tube surface and then heating at elevated temperature to create a porous coating having a large number of nucleation sites. The properties of the tube are as follows:

Outside diameter = 15.8 mm

Inside diameter = 11.6 mm

Porous metal film thickness = 0.025 mm (approximately)

Table 2. COMPUTER/DATA ACQUISITION ASSIGNMENT

Thermocouple Description	Channel	Array in code
Vapor	00	T(0)
Vapor	01	T(1)
Vapor	02	T(2)
Liquid	03	T(3)
Liquid	04	T(4)
Tube 1, No. 1	40	T(5)
Tube 1, No. 2	41	T(6)
Tube 1, No. 3	42	T(7)
Tube 1, No. 4	43	T(8)
Tube 1, No. 5	44	T(9)
Tube 1, No. 6	45	T(10)
Tube 2, No. 1	46	T(11)
Tube 2, No. 2	47	T(12)
Tube 2, No. 3	48	T(13)
Tube 2, No. 4	49	T(14)
Tube 2, No. 5	50	T(15)
Tube 2, No. 6	51	T(16)
Tube 3, No. 1	52	T(17)
Tube 3, No. 2	53	T(18)
Tube 3, No. 3	54	T(19)
Tube 3, No. 4	55	T(20)
Tube 3, No. 5	56	T(21)
Tube 3, No. 6	57	T(22)
Tube 4, No. 1	58	T(23)
Tube 4, No. 2	59	T(24)
Tube 4, No. 3	60	T(25)
Tube 4, No. 4	61	T(26)
Tube 4, No. 5	62	T(27)
Tube 4, No. 6	63	T(28)
Tube 5, No. 1	64	T(29)
Tube 5, No. 2	65	T(30)
Tube 5, No. 3	66	T(31)
Tube 5, No. 4	67	T(32)
Tube 5, No. 5	68	T(33)
Tube 5, No. 6	69	T(34)

Table 2 (contd.). COMPUTER/DATA ACQUISITION ASSIGNMENT

Amperage Sensors Description	Channel	Array
Tube 1	30	Amp(0)
Tube 2	31	Amp(1)
Tube 3	32	Amp(2)
Tube 4	33	Amp(3)
Tube 5	34	Amp(4)
Active	35	Amp(5)
Active	36	Amp(6)
Active	37	Amp(7)
Active	38	Amp(8)
Active	39	Amp(9)
Auxiliary Heaters	25	Amp(10)
Simulation Heaters	26	Amp(11)
Voltage Sensor Description	Channel	Array
Instrumented Active	27	Volt(0)
Simulation Heaters	28	Volt(1)
Auxiliary Heaters	29	Volt(2)

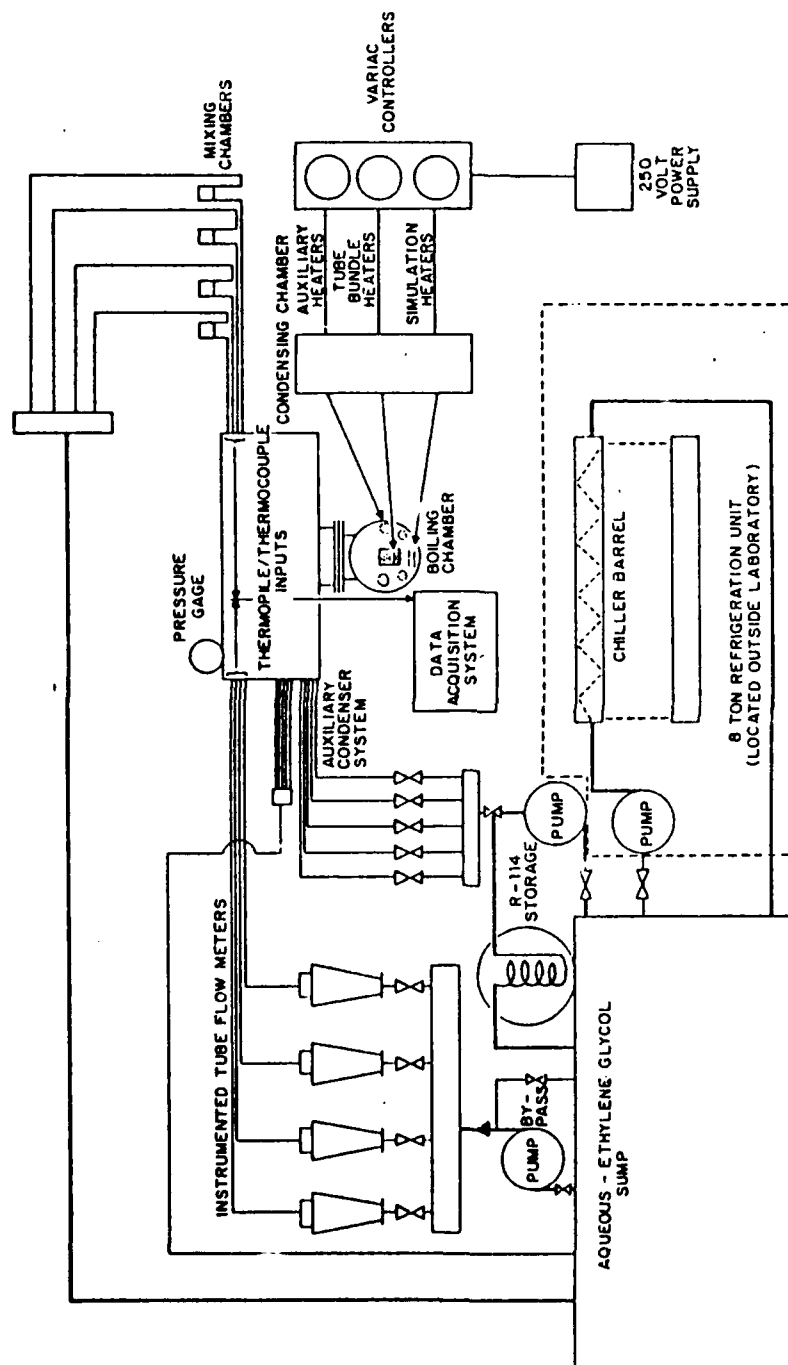


Figure 1. Schematic View of the Apparatus

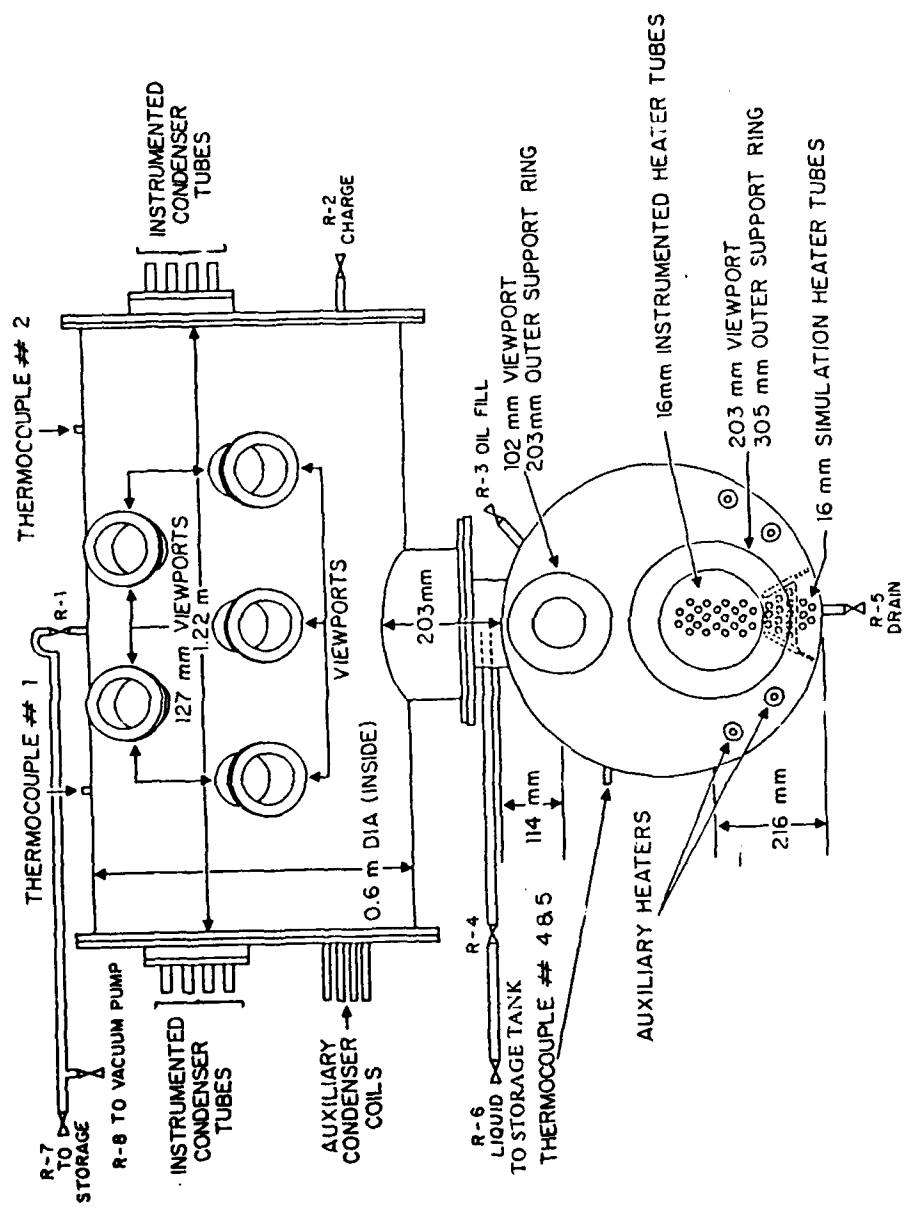


Figure 2. Evaporator/Condenser Schematic

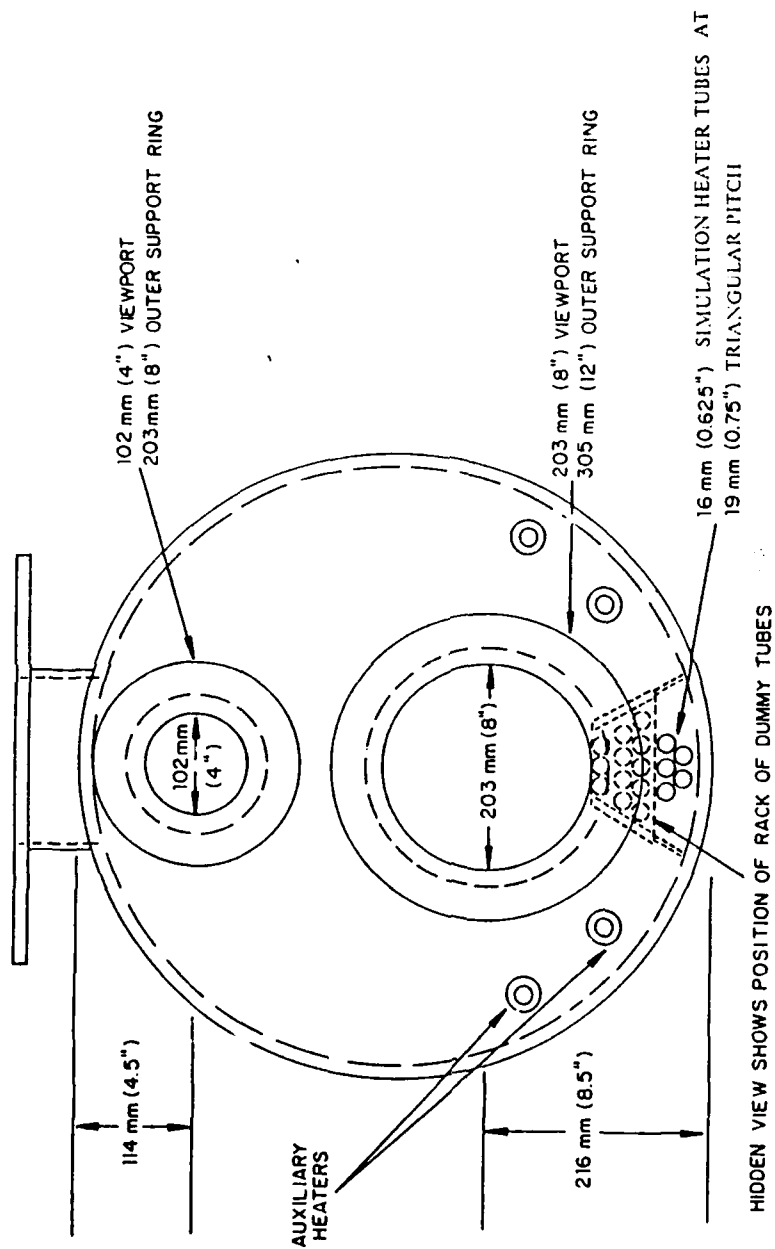


Figure 3. Front View of Evaporator

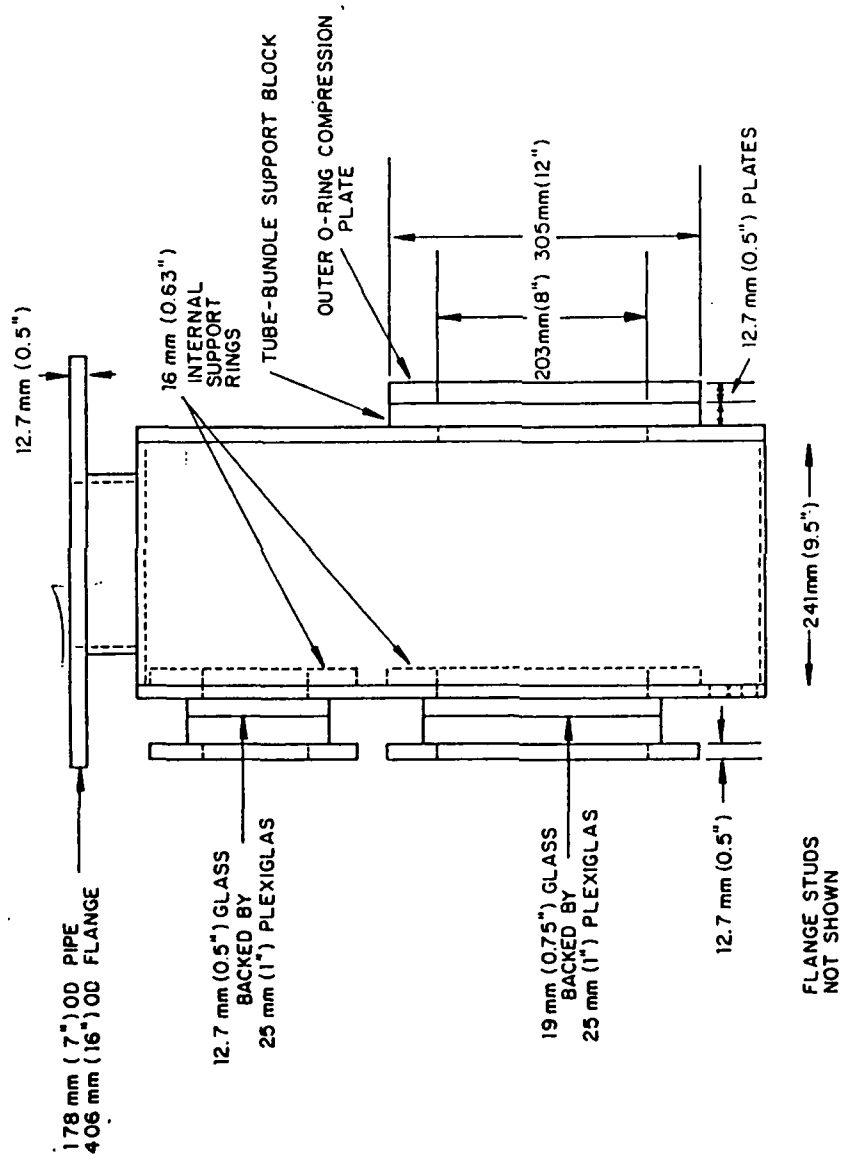


Figure 4. Side View of Evaporator

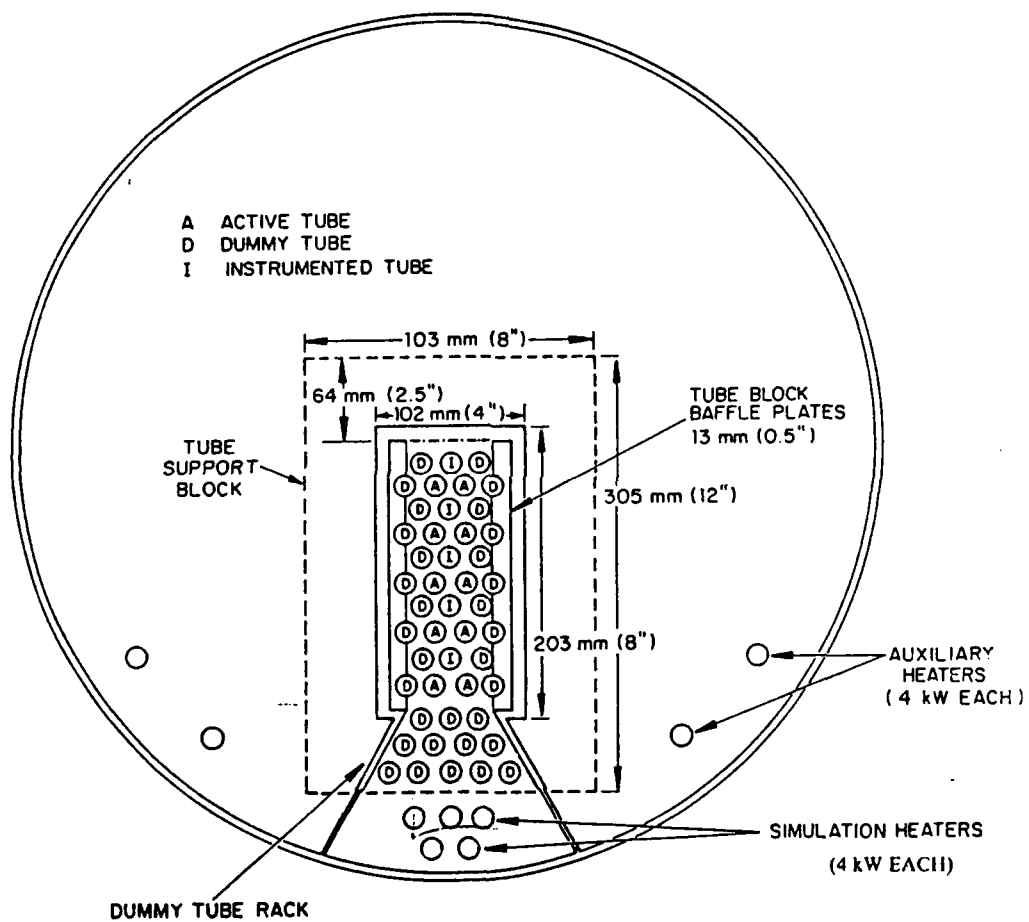
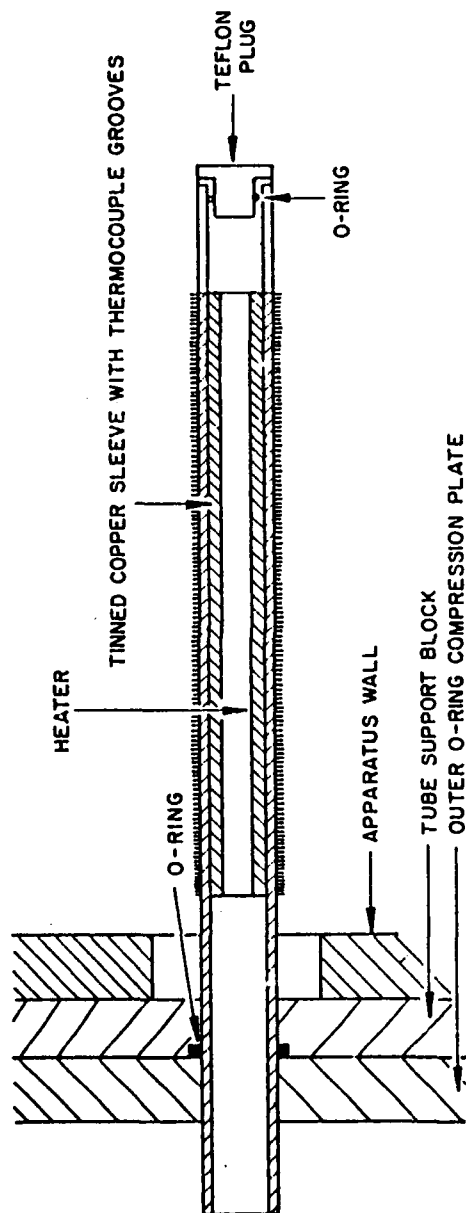
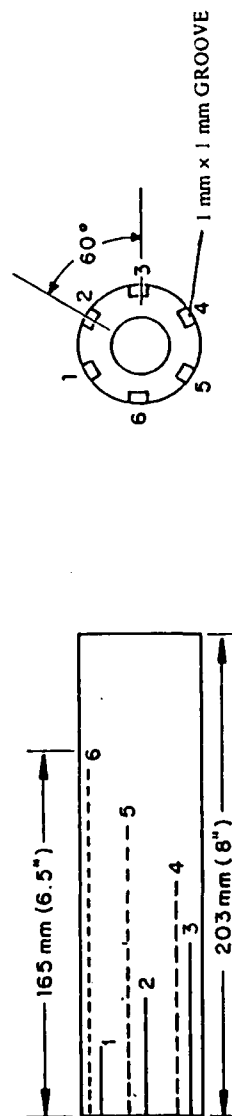


Figure 5. Sectional View of Evaporator Showing Tube Bundle



(a) BUNDLE HEATER TUBE SECTIONAL VIEW



(b) THERMOCOUPLE LOCATIONS ALONG HEATED LENGTH

Figure 6. Thermocouple Locations on an Instrumented Boiling Tube and Tube Section View

IV. EXPERIMENTAL PROCEDURES

A. MANUFACTURE OF INSTRUMENTED EVAPORATOR TUBES

The first step in this process was to machine the tubes and sleeves to specified dimensions. Two different techniques were used to manufacture the tubes. In the first technique (described and used by Anderson [Ref. 3]), type-T copper-constantan thermocouples were positioned in grooves machined on the copper sleeve and a cartridge heater was inserted inside the copper sleeve. The thermocouples were secured in place by bending over the edges of the grooves at 2.5 cm intervals with a blunt punch.

All surfaces to be soldered were then brushed with a liquid flux solution and after approximately one minute, the excess flux solution was removed with a cloth. The evaporator tube was placed vertically in a 12 inch long furnace. The cartridge heater in the sleeve was connected to a voltage controlling rheostat. A multiple channel Omega digital indicator was used to monitor the inside temperature of tube and the outside temperature of the copper sleeve (using one of the sleeve thermocouples). The furnace temperature and the voltage to the cartridge heater were adjusted until the temperature of both the sleeve and tube were approximately 200 C. This temperature was maintained while solder was applied to the outside of the copper sleeve and the inside of the tube. This eutectoid solder consisted of 40% tin and 60% lead and its melting point was 190 C. The temperature was monitored very carefully so that the melting point of the teflon thermocouple insulation (260 C) was not exceeded. After this process, the copper sleeve was inserted into the evaporator tube. A temporary friction fitting aluminum plug, which extended in the evaporator tube by 1 inch, served as a "stop" for the sleeve. A copper end cap was soldered in position by using additional heat and then power was secured. The evaporator tube was left to cool.

Five instrumented finned evaporator tubes were fabricated using this technique. They were manufactured by Wolverine tube company and had a 9.3 mm inside diameter. Upon installation of these tubes and operation of the system, however, it was observed that the wall temperatures were not homogeneous. At a heat flux of 95 kW/m^2 , the highest difference between maximum and minimum thermocouple readings was obtained as 25.3 C and the lowest difference was 9.1 C. This type of tube had a very thin copper sleeve (about 1.5 mm thick). It was thought that this short distance between thermocouples and heater was the cause of the large temperature difference and

nonhomogeneity. With this in mind, the manufacturing process was repeated but a smaller cartridge heater (3.17 mm vs. 6.35 mm in diameter) was used. The new procedure showed that even with the smaller diameter heater, the problem was not eliminated. In order to find the source of the problem, three sections were cut from one tube (top, bottom and middle). These cross sections were prepared and examined in the Materials Science laboratory. Pictures of the cross sections were taken under high magnification using an electron microscope. It was observed that the contact between the inside tube wall and copper sleeve was very poor. The inside walls of the Wolverine finned tubes were not quite round and the solder did not fill the entire gap between the wall and the sleeve. Figure 7 shows an air gap caused by a poor solder bond.

It was here that the second manufacturing technique was tried using Wieland finned tubes which had a larger inside diameter and more round inside surface. The technique was similar to the first except for the soldering process. The second technique used a special solder (SWIF) which has the solder (50% tin, 50% lead) and flux in a paste form. The inside tube wall and the surface of the copper sleeve were cleaned. SWIF was applied on both surfaces. The copper sleeve was then inserted into the tube and an aluminum plug was used to position the copper sleeve properly. The evaporator tube was then placed in a 12 inch furnace horizontally and all thermocouples were connected to a multi-channel Omega digital indicator. The furnace was heated up and temperatures were observed from the indicator. When the temperature of the evaporator tube reached 200 C (which is slightly above the melting point of SWIF), the tube was taken out and quenched immediately at the cable end using a cloth saturated with water. The evaporator tube was then placed vertically with the cable end at the bottom and was heated by a torch. Temperatures were maintained near the melting point of the eutectoid solder. Additional solder was then applied slowly from the top end until no liquid solder flow was observed inside of the tube. The tube was then allowed to cool to room temperature. During this soldering process, a water-saturated cloth was held at the bottom of the tube to prevent solder leakage from the cable end and to hold the copper sleeve in position. This second technique resulted in much smaller wall temperature variations (within 2.5 C at maximum heat flux).

B. INSTALLATION OF EVAPORATOR TUBES AND TUBE SUPPORT BLOCK

The front-viewing window was removed carefully in order to prevent damage to the window (cracks, chips etc.). The nuts for the tube support block were unscrewed and the tube support block was removed, paying particular attention not to disturb the

thermocouple extensions in the kettle-reboiler. The tube support block contains 5 instrumented evaporator tubes, 12 active heated evaporator tubes and 18 dummy evaporator tubes. Only instrumented and active evaporator tubes penetrate through the block allowing the thermocouple and heater wires to come out from the test section. O-rings were placed on the tubes between the tube support block and the stainless-steel backing plate to prevent problems due to loss of vacuum.

The evaporator tubes were installed in the block without tightening the backing plate nuts and then the block was guided into the kettle boiler. The tube support block bolt holes were aligned to the appropriate bolts on the evaporator and all nuts were placed and tightened. Then the front viewing window gasket was replaced with a new one and the window was adjusted and tightened appropriately. First the window gasket was placed, then the glass window and Lexan plate (they have same diameter) were positioned on the gasket. In this configuration, the Lexan plate must be at the outside. Finally, the outer support ring was placed on the Lexan plate and all bolts were tightened by hand. Very small and equal torques were applied circumferentially to the nuts using a wrench. In order to protect the sensitive glass window, excess torque must not be applied and the support ring must not be tightened with a missing nut or bolt. All tubes then were pushed forward to touch the front viewing window to obtain vertical alignment of the evaporator tubes. The backing plate was then tightened and the O-rings compressed.

C. SYSTEM EVACUATION

First of all, the system was isolated from the atmosphere using a Seargent Welch 10 SCFM vacuum pump. Figure 2 displays necessary valves for system evacuation, freon removal or freon fill. According to this figure, the valves R-1 and R-8 were opened and all other valves were closed during operation of the vacuum pump. Approximately three to four hours later, 29 inches mercury vacuum was reached. Valves R-1 and R-8 were closed, and the vacuum pump secured. The system was observed for at least 10 hours with no noticeable pressure drop. Unfortunately, sometimes the vacuum could not be held at 29 inches mercury. Large leaks caused by the gasket of the boiler-condenser main flange were detected by using 15 psi air. Air was added thru valve R-2 and the leaks were found using their sound. The foam detection technique can also be used with air for smaller leaks. Some small leaks caused by the window gaskets or valves were detected using freon vapor and a sensitive freon detector. In this detection scheme, the system was filled with R-114 vapor up to 5-7 psi by using valve R-2. Then a freon

detector was used to find the leaks. After finding all the leaks and the vacuum was held for a sufficient time (at least 10 hours), the system was ready to be filled with freon.

D. FREON FILL

Only R-114 was used for the experiments. Once the cooling sump was cooled to a temperature less than -10 C using the 8 ton refrigeration unit which was described in the previous Chapter, both instrumented and auxiliary condenser pumps were turned on and both condensers were placed in operation to cool the system. At that time, the storage tank pressure was 13 psi and the system was under 29 inches mercury vacuum. Then valves R-6 and R-4, which are located at the bottom of the storage tank and at the back side of the boiler, were opened to start the transfer of liquid R-114. When the pressure of the storage tank and system was equal, transfer was complete. This pressure was between 5 and 8 inches mercury vacuum at the -20 C sump temperature. Both pumps were then secured and valves R-6 and R-4 were closed. The liquid level mark, which was scratched on the rear section of the evaporator wall (can be seen from upper view glass of the evaporator), was checked and additional freon was charged from the liquid side of the purchased cylinder container while the system was under vacuum. Again valve R-2 was used to fill additional freon.

E. FREON REMOVAL

R-114 had to be removed from the system for maintenance and tube replacement. A storage tank is available to store R-114 during these periods.

While the sump tank temperature was being cooled to less than -10 C, valves R-7 and R-8 were opened and the vacuum pump was turned on to put the storage tank under vacuum. When the vacuum reached 29 inches mercury, and the sump temperature was less than -10 C, the vacuum pump was stopped, R-8 was closed and coolant was pumped from the sump through the storage tank condenser. Valve R-1 was then opened and freon vapor reached the storage tank and condensed on the condenser coil. Actually this process takes more time than freon filling does, but if heaters are used to increase the vapor generation from boiler, the time can be reduced. If the heaters are being used, the system pressure must not exceed maximum design pressure (30 psi) and also the heaters must always be submerged in liquid. When the pressure of the system and storage tank was equal, the transfer was over. Valves R-1 and R-7 were then closed.

F. GENERAL OPERATION

For operating the system, the first step was to run the 8 ton refrigeration unit for two hours which provided a sump temperature of -10 C or less. The system pressure was 12/13 psig and the saturation temperature of freon was much higher than the test saturation temperature, according to this pressure. A gradual increase of the cooling through the condenser was provided until a saturation temperature of 2.2 C was achieved at the beginning of each run. When the freon reached this saturation temperature, the saturation pressure was slightly below 0 psig.

When saturation conditions were obtained and the system was stabilized at these conditions, the desired number of tubes were heated up to a surface heat flux of 70-100 kw/m^2 by using an adjustable rheostat. Boiling conditions were maintained for 30 minutes. Decreasing heat flux runs were then applied in steps as described in Chapter V. For each flux level, saturation conditions were maintained for at least five minutes by adjusting the coolant flow rate passing through the condenser. At least five minutes was necessary to make sure that system equilibrium was attained.

G. OIL ADDITION

The mass of R-114 in the evaporator was calculated to be 60.3 kg at -15 C when it was filled up to the level mark. The experiments were made by using pure R-114 and R-114 oil/mixtures. The required amount of oil was added to freon successively. One percent oil, 603 gr, was measured as 670 ml. Once the system pressure was reduced by at least 5 inches mercury vacuum by using the condenser cooling, the oil was poured into a measuring cup and a hose which was connected to valve R-3, was primed with oil. The open end of the hose was closed carefully and submerged into the oil without having any contact with air. The valve R-3 was opened and the oil was syphoned from the cup by vacuum. The scale of measuring cup was observed carefully to insure the correct amount of oil was added to the freon. Valve R-3 was closed after a sufficient amount of oil was syphoned.

H. DATA-REDUCTION PROCEDURES

The data reduction program "DRP4" was used as software in this investigation. The capabilities of the program were explained and the entire listing of the program was provided by Anderson [Ref. 3] in his thesis.

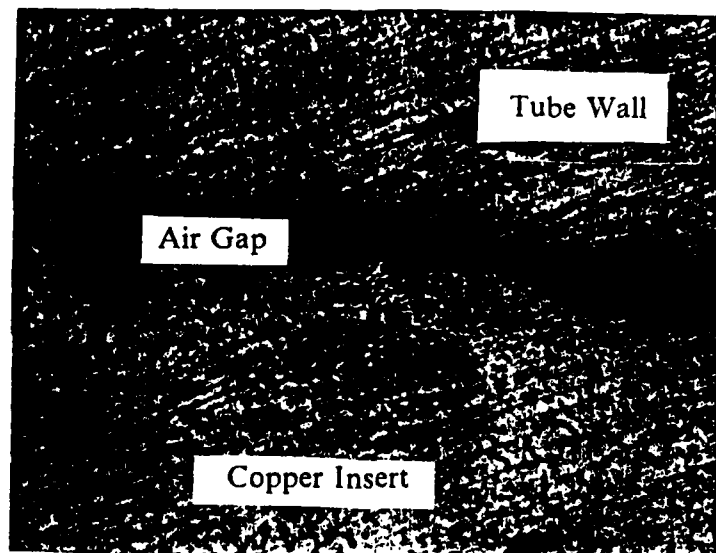


Figure 7. Photomicrograph Showing Air Gap Between Tube and Copper Insert (Magnification 200X)

V. RESULTS AND DISCUSSION

A. GENERAL DESCRIPTIONS

The finned and High Flux tube bundles were tested in R-114 and R-114/Oil mixtures at a boiling temperature of 2.2 C and their respective performances were calculated. Six oil concentrations were used in this investigation: 0%, 1%, 2%, 3%, 6% and 10% by mass.

The data sets were taken from five instrumented tubes which were numbered from top to bottom as 1, 2, 3, 4, and 5. Figure 8 shows the position of the instrumented tubes in the bundle.

All runs were performed using the same surface aging technique. In this technique, refrigerant was boiled for 30 minutes using a maximum power of $75\text{--}100\text{ kW/m}^2$ and data were taken in steps during decreasing heat flux to a minimum flux of $1\text{--}2\text{ kW/m}^2$. Either ten or nine steps were used over this heat flux range and data were taken at each step. This surface aging technique closely simulated a continuously operating air-conditioning system. This decreasing heat flux served to eliminate the hysteresis effects that occur in nucleate boiling. 42 runs were performed for each tube type and the results were stored as data and plot files. File names were used to identify tube type, oil amount in freon, run type and the number of tubes used. Each file name starts with either "FIN" or "HIF" which represents finned and High Flux tube types respectively. The letter "D" indicated a run utilizing a decreasing heat flux. One or two numbers after these letters show the percentage oil in freon by mass and the last number stands for the operated number of tube. The last number varies from one to seven, six and seven representing whole bundle and bundle plus five simulated tube rows in operation, respectively. For example, file "HFD35" represented High Flux tubes, decreasing run, three percent oil in freon and five instrumented tubes in operation. Plot file names were created just utilizing the letter "P" in front of the data file name. The complete file names and details about files are shown in Table 8 in Appendix A.

All graphs, with one exception, were plotted as heat flux versus wall superheat in this Chapter. Heat flux was obtained by dividing electrical power output by surface area. Root diameters were used to calculate surface area of finned and High Flux tubes. The wall superheat was the difference between the outside tube temperature and the saturation temperature. The inside tube temperature was obtained from the average of

six thermocouple readings and the temperature drop across the wall thickness was calculated. Then tube outside temperature was obtained by subtracting the temperature drop from the tube inside temperature. This is shown in Appendix B.

Even though the same technique was used to manufacture both the finned and High Flux tubes, the temperature variations on the finned tube wall were more homogeneous than the High Flux tubes. As a natural result of this, larger uncertainties were associated with high flux tube data. Tables 3 and 4 show the thermocouple temperature readings on the wall of the finned and High Flux tubes respectively.¹

Table 3. FINNED TUBE WALL TEMPERATURE READINGS FROM 6 THERMOCOUPLES AT A HEAT FLUX OF 90 KW/M²

Tube #	TC1 (C)	TC2 (C)	TC3 (C)	TC4 (C)	TC5 (C)	TC6 (C)	AVE. (C)
1	9.68	10.01	10.18	10.41	10.40	10.06	10.12
2	10.03	10.06	10.29	9.64	10.21	10.14	10.07
3	10.25	9.84	10.03	10.57	10.90	11.10	10.45
4	10.22	9.88	10.33	10.44	-99.99	11.34	10.44
5	9.84	9.67	11.44	11.39	12.16	11.49	11.00

Table 4. HIGH FLUX TUBE WALL TEMPERATURE READINGS FROM 6 THERMOCOUPLES AT A HEAT FLUX OF 75 KW/M²

Tube #	TC1 (C)	TC2 (C)	TC3 (C)	TC4 (C)	TC5 (C)	TC6 (C)	AVE. (C)
1	5.93	6.92	5.49	4.97	5.62	6.05	5.83
2	5.32	4.82	5.26	6.27	6.27	5.77	5.62
3	5.74	5.60	5.78	6.95	7.77	8.41	6.71
4	6.55	6.82	7.29	7.27	7.50	7.95	7.23
5	6.37	6.99	5.77	5.50	5.83	7.05	6.25

B. R-114 BOILING FROM FINNED TUBE BUNDLE

The performance of a single finned tube within the bundle (but with no other tubes on) is shown in Figure 9 with typical uncertainty bands in wall superheat. The uncertainties in wall superheat were calculated as $\pm 20\%$ and $\pm 5.5\%$ for low and high heat

¹ -99.99 was used to indicate a defective thermocouple.

flux levels respectively. Figure 10 shows the variation of tube number one performance with an increasing number of heated tubes in the bundle. When the top two tubes were operated, tube number one was influenced by tube number two and its performance increased markedly, especially at low heat flux levels. The reason was the convective effect on the upper tube by the bubbles created from the lower tube. Performance of tube number one continued to increase with the addition of tubes three, four and five. A second significant increase was observed when the bundle was operated. The side bundle tubes became active and produced bubbles. The instrumented tubes were influenced by the bubbles, produced by the bottom tubes and the side bundle tubes. A very dense bubble flow was created around the tubes and the convective effect of the bubbles increased the heat transfer. The effect of simulated tubes on the top tube was not extreme. Maximum enhancement was obtained at the lowest applied heat flux level (1.5 kW/m^2). The influence of the lower bundle of heated tubes disappeared above a heat flux of 50 kW/m^2 where all the data converged. The performance of each tube in the bundle was increased by increasing the number of heated tubes below them. The performance curves of each instrumented tube in the bundle also converged at large heat fluxes. Figure 11 shows the performance curves of the five instrumented tubes during bundle operation and indicates the above result. Simulation heaters were used to simulate 5 additional rows of tubes in the bundle but their effect was not significant, especially for the upper instrumented tubes. Figure 12 gives the performance results of bundle operation with the addition of the simulation heaters. Notice that the obtained curves are similar to the bundle operation curves given in Figure 11. The performance enhancements due to the bundle operation were calculated using the ratio of the average bundle heat transfer coefficient to the single tube heat transfer coefficient. They were obtained as 0.96, 1.45, 1.92 for a heat flux of 70, 10 and 4 kW/m^2 respectively. The enhancement effect of the bundle was nearly zero for high heat fluxes and the performance of the bundle approached that of the single tube.

C. R-114/OIL MIXTURES BOILING FROM FINNED TUBE BUNDLE

The effect of oil additions to top tube performance of the bundle was compared with single tube performance in pure R-114. After a 1% oil addition, the top tube performance increased significantly over the entire heat flux range. Single tube operation with various oil concentrations (up to 10%) showed that the performance was always better than no oil condition. Above a heat flux of 10 kW/m^2 , the increased performance was observed up to 3% oil. In other words, maximum enhancement was obtained with 3%

oil and at the maximum heat flux. The wall superheat decreased around 2 K in this condition. For 6 and 10% oil addition, performance slowly decreased if compared with 3% oil performance but it continued to be better than pure R-114. Figure 13 shows the variation of the performance of tube number one with various oil concentrations.

The bundle results were nearly parallel to the single tube results. Overall bundle performance increased up to a 3% oil addition. 6% and 10% oil concentrations showed better bundle performance above a heat flux of 10 kW/m^2 . Below this heat flux, bundle performance deteriorated. The top tube performance from bundle operations of each oil addition closely follows the above trends and it was plotted in Figure 14 and used to represent the overall bundle performance relatively. Heat transfer results of the bundle are shown for R-114 with each oil addition in Figure 15 through Figure 19. Bundle heat transfer coefficients and enhancement ratios for pure R-114 and R-114/oil mixtures are tabulated in Tables 5 and 6 for smooth tubes (from Anderson [Ref. 3]) and finned tubes respectively. The enhancement ratios for the bundle were obtained by dividing the average bundle heat transfer coefficient for a R-114/Oil mixture to the average bundle heat transfer coefficient for pure R-114. A heat flux of 30 kW/m^2 was chosen for calculation because this value is near actual refrigerant evaporator conditions and the enhancement ratio due to the oil concentration was always bigger than unity. Therefore, oil contamination actually assists in heat transfer at this level of heat flux.

During bundle operation above a heat flux level of 50 kW/m^2 , the ordinary bubble flow pattern was not observed. Instead, bubbles around the tubes fluctuated up and down in an oscillatory fashion with a certain frequency due to fluid motion in the kettle-reboiler. This fluctuation was significant at the bottom tubes of the bundle and became more observable with increasing oil contamination. Once the bubbles were produced, they could not rise freely and stayed around the tube for a short period of time. Therefore a negative effect of this kind of bubble behaviour to the performance was expected but no significant deviation was recognized in performance (ie. the slope of the performance curves did not change significantly between heat flux levels). Another observation from R-114/Oil mixtures was the existence of foaming. Foaming was increased by increasing heat flux, the number of heated tubes and the oil amount. The above discussion indicates that the bundle performance increased at the high heat flux levels. This can be partly related to increased foaming and higher flow circulation rate.

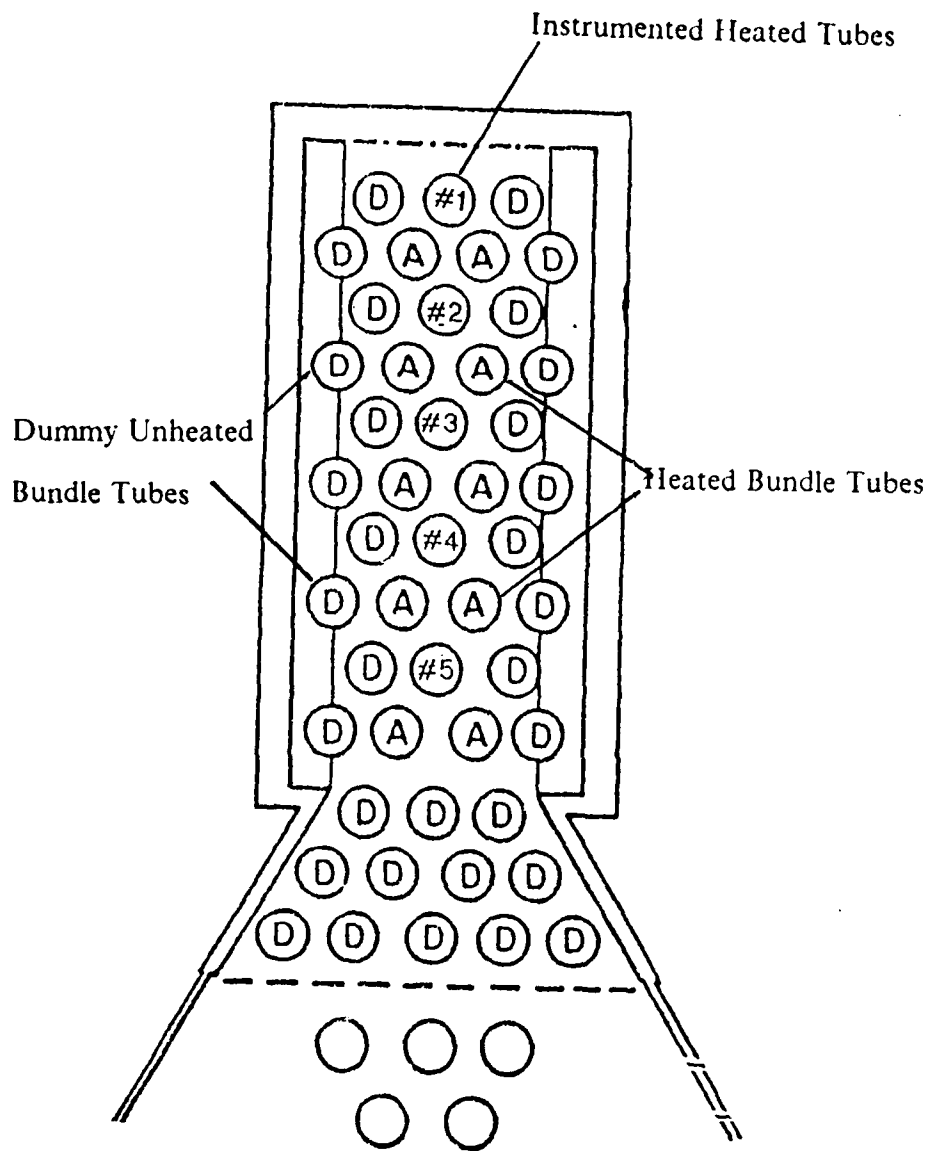


Figure 8. Position of Instrumented Tubes in the Tube Bundle

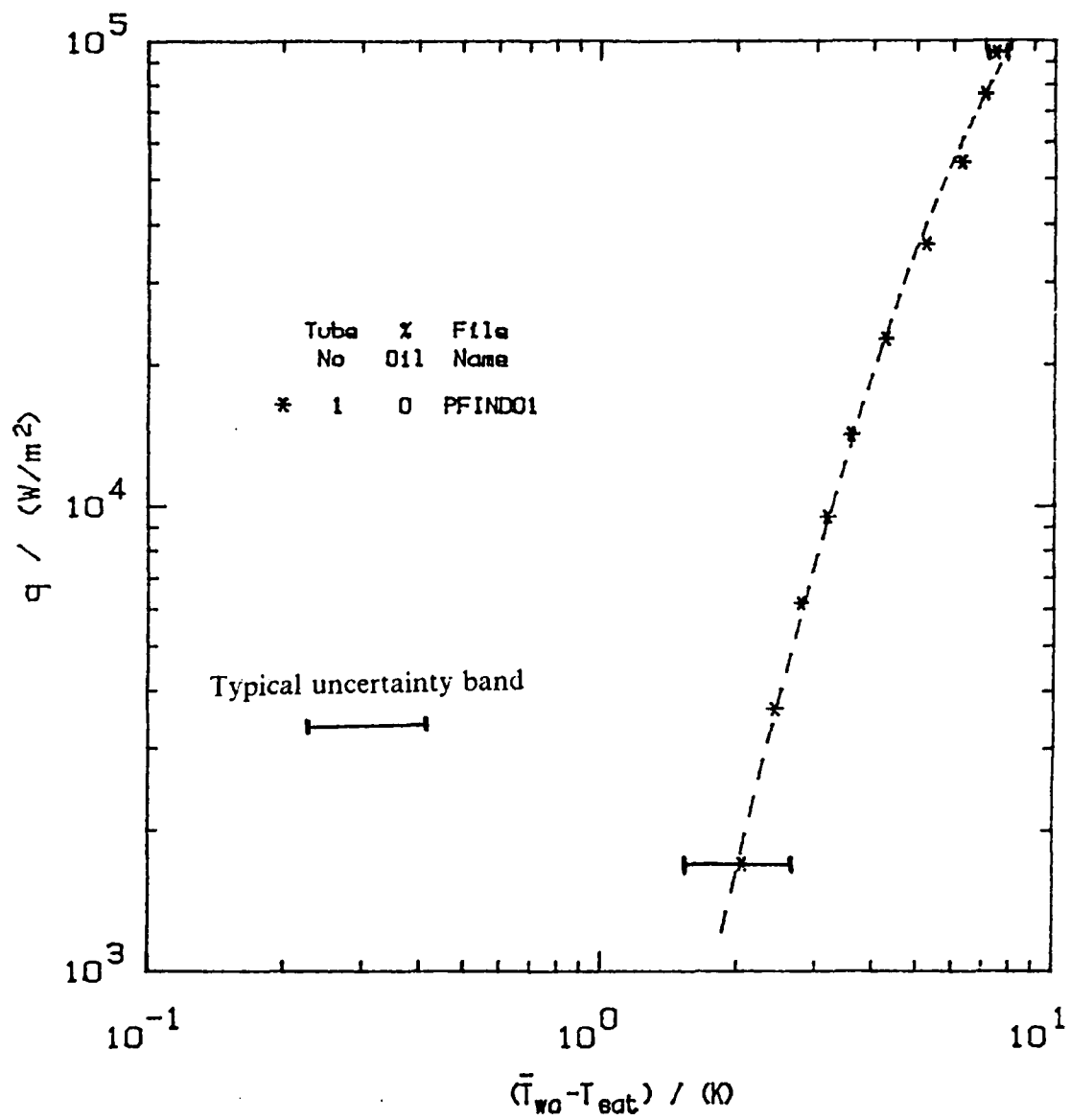


Figure 9. Single Finned Tube Performance in R-114 within Finned Tube Bundle

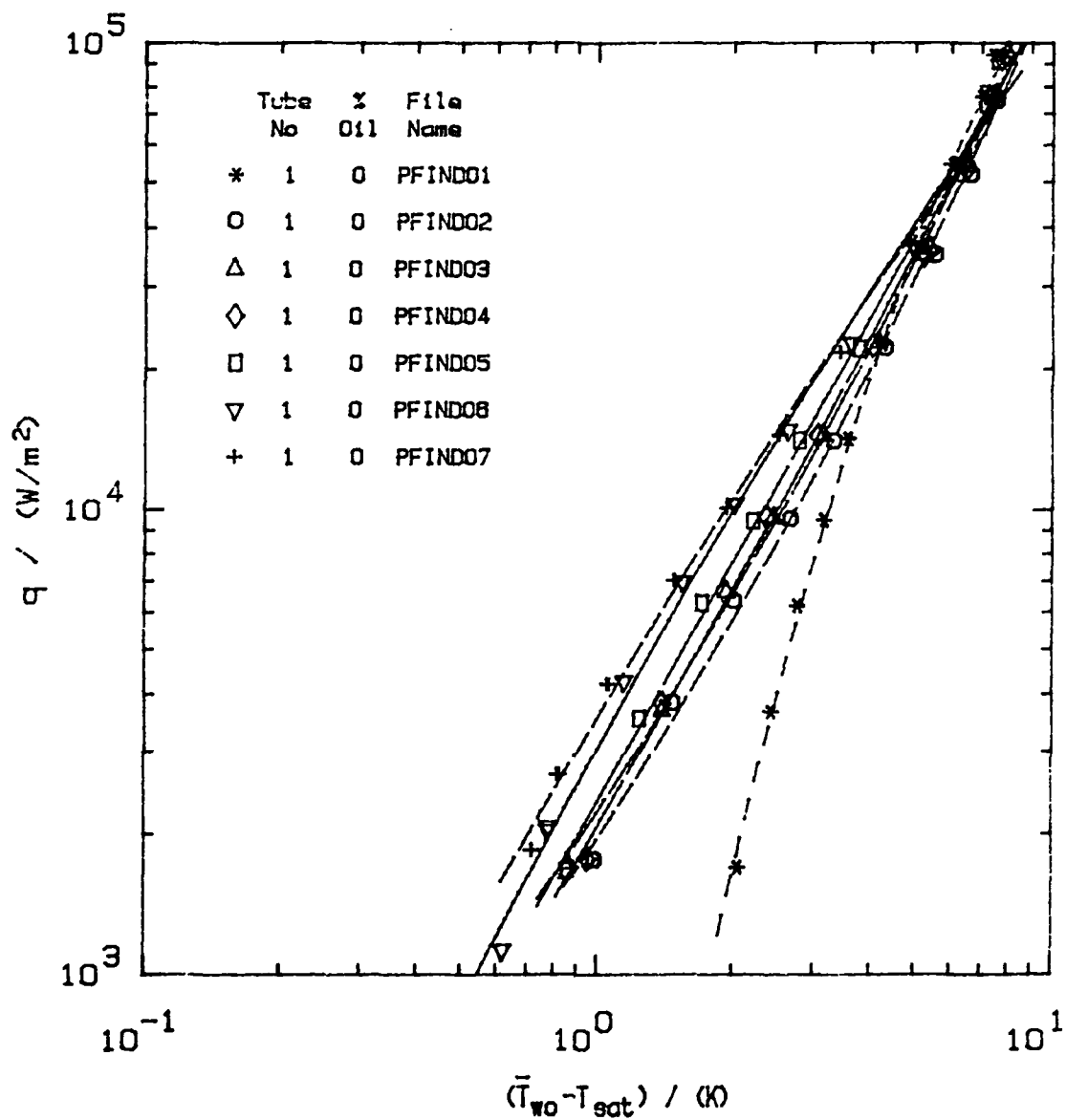


Figure 10. Performance Variation of Tube Number One in R-114 when Influenced by Increasing Number of Heated Tubes in Finned Tube Bundle

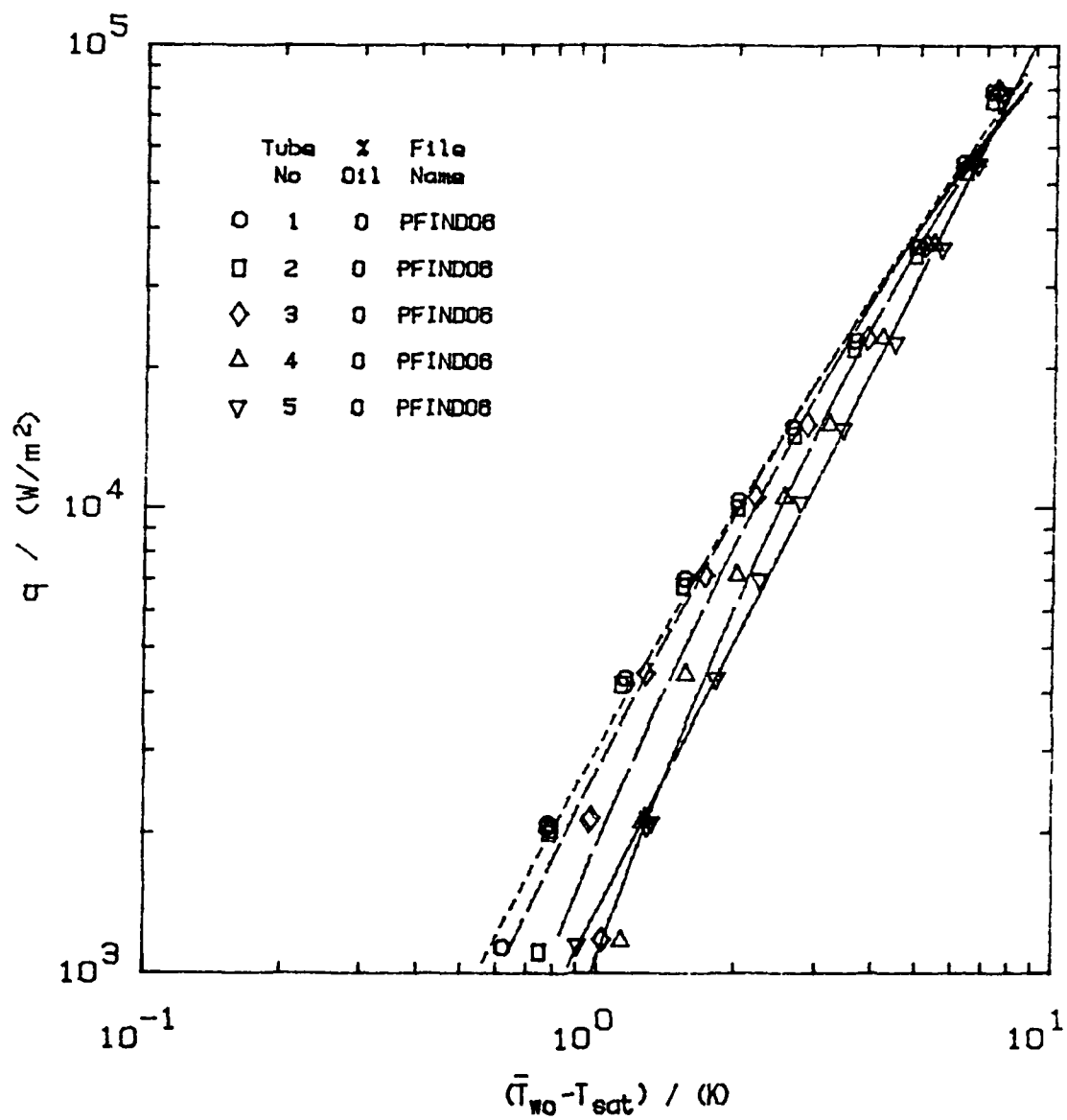


Figure 11. Heat Transfer Performance Results of Finned Tube Bundle in Pure R-114

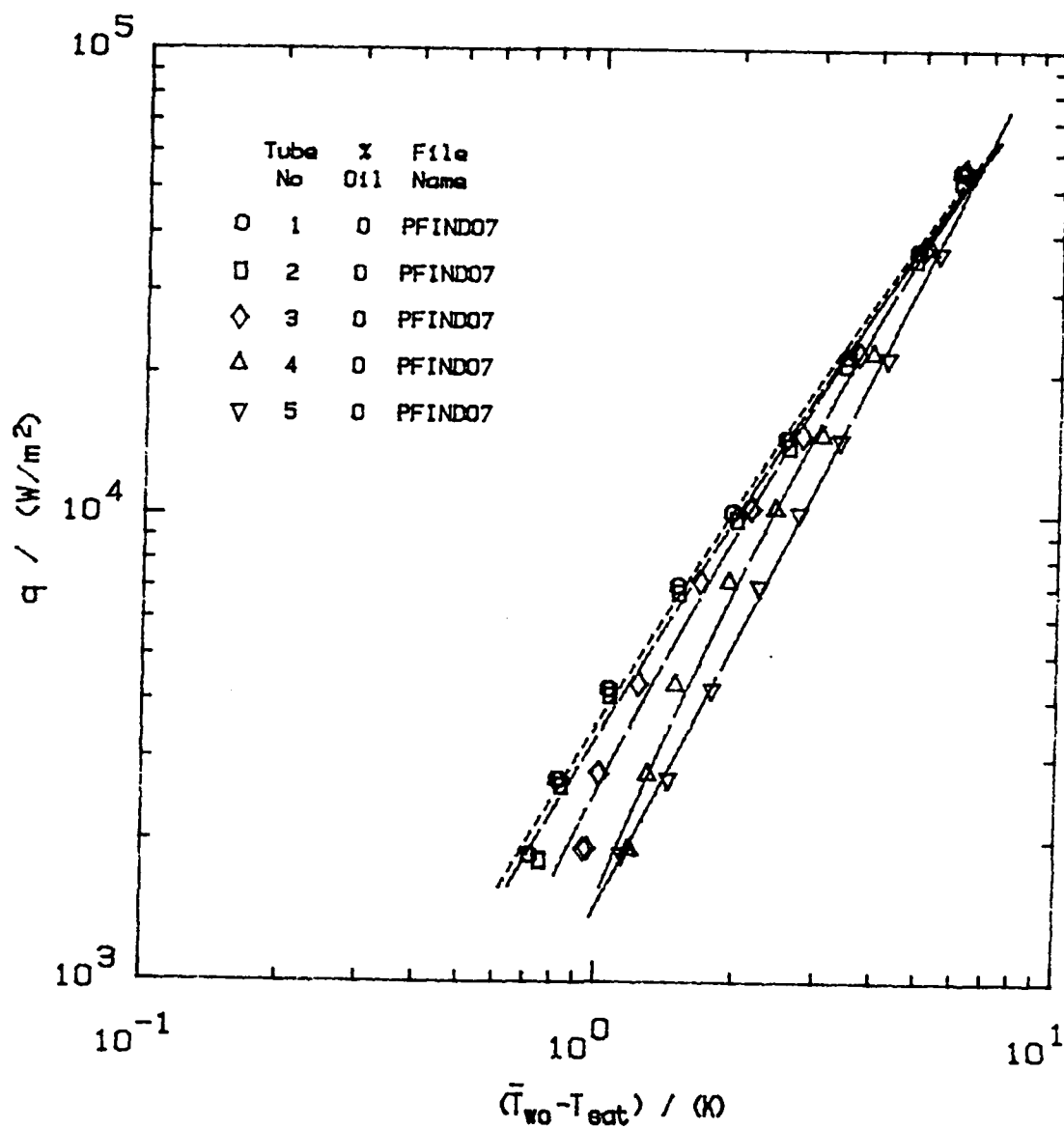


Figure 12. Heat Transfer Performance Results of Finned Tube Bundle with Simulation Heaters in Pure R-114

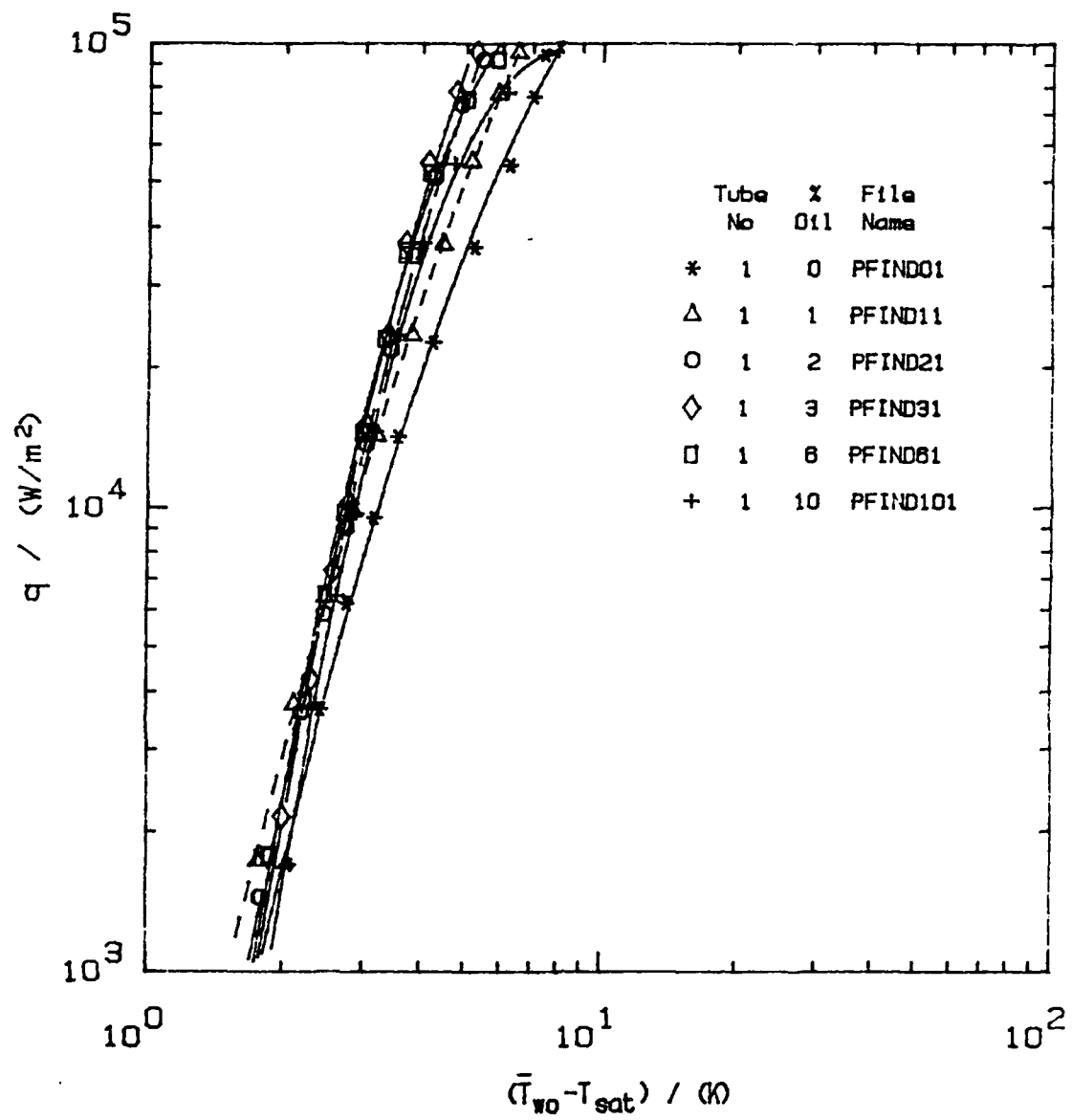


Figure 13. Performance Variation of Tube Number One with Variation of Oil Concentrations

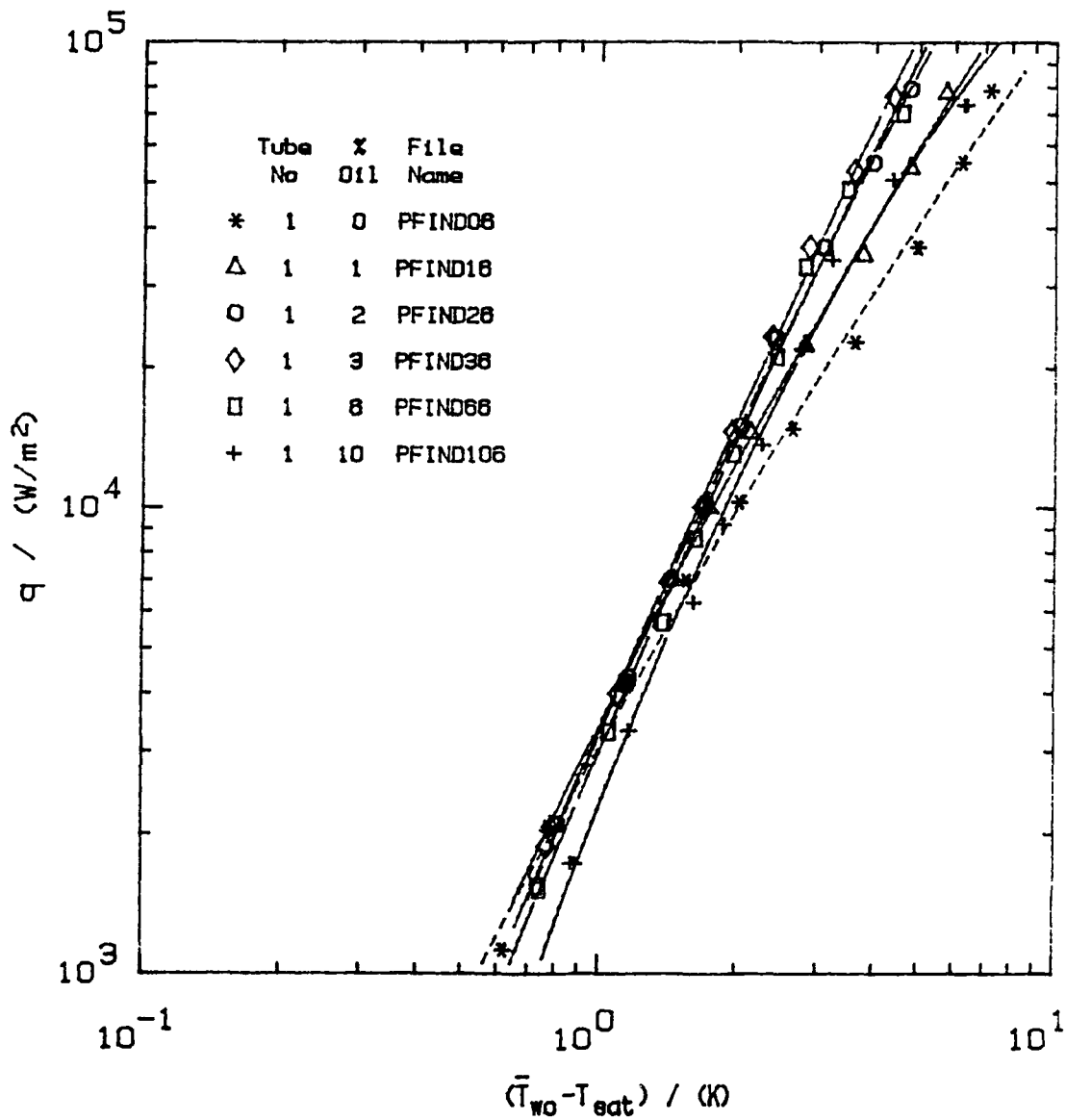


Figure 14. Performance Variation of Tube Number One with Variation of Oil Concentrations During Finned Tube Bundle Operation

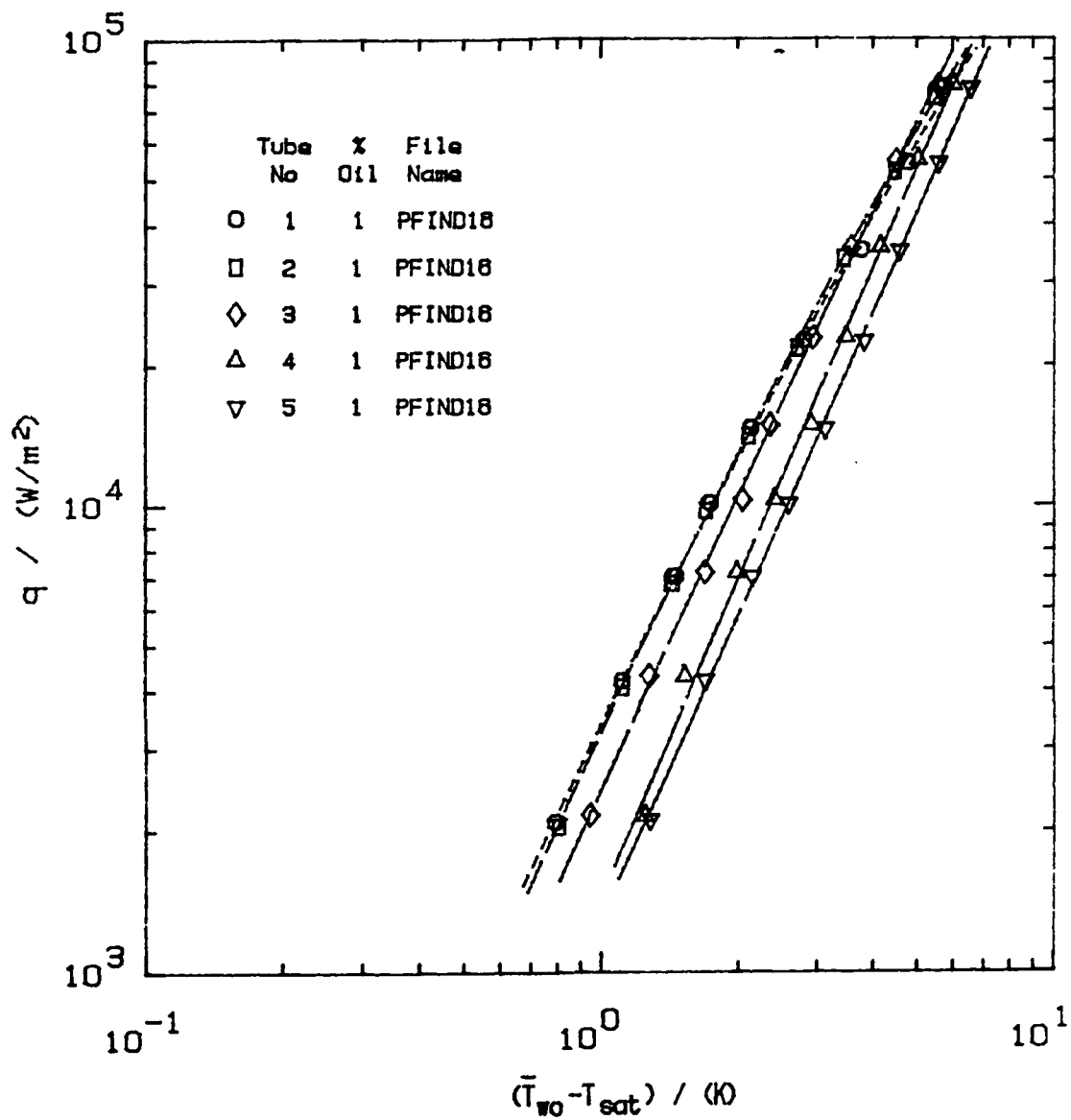


Figure 15. Heat Transfer Performance Results of Finned Tube Bundle with 1% Oil Concentration

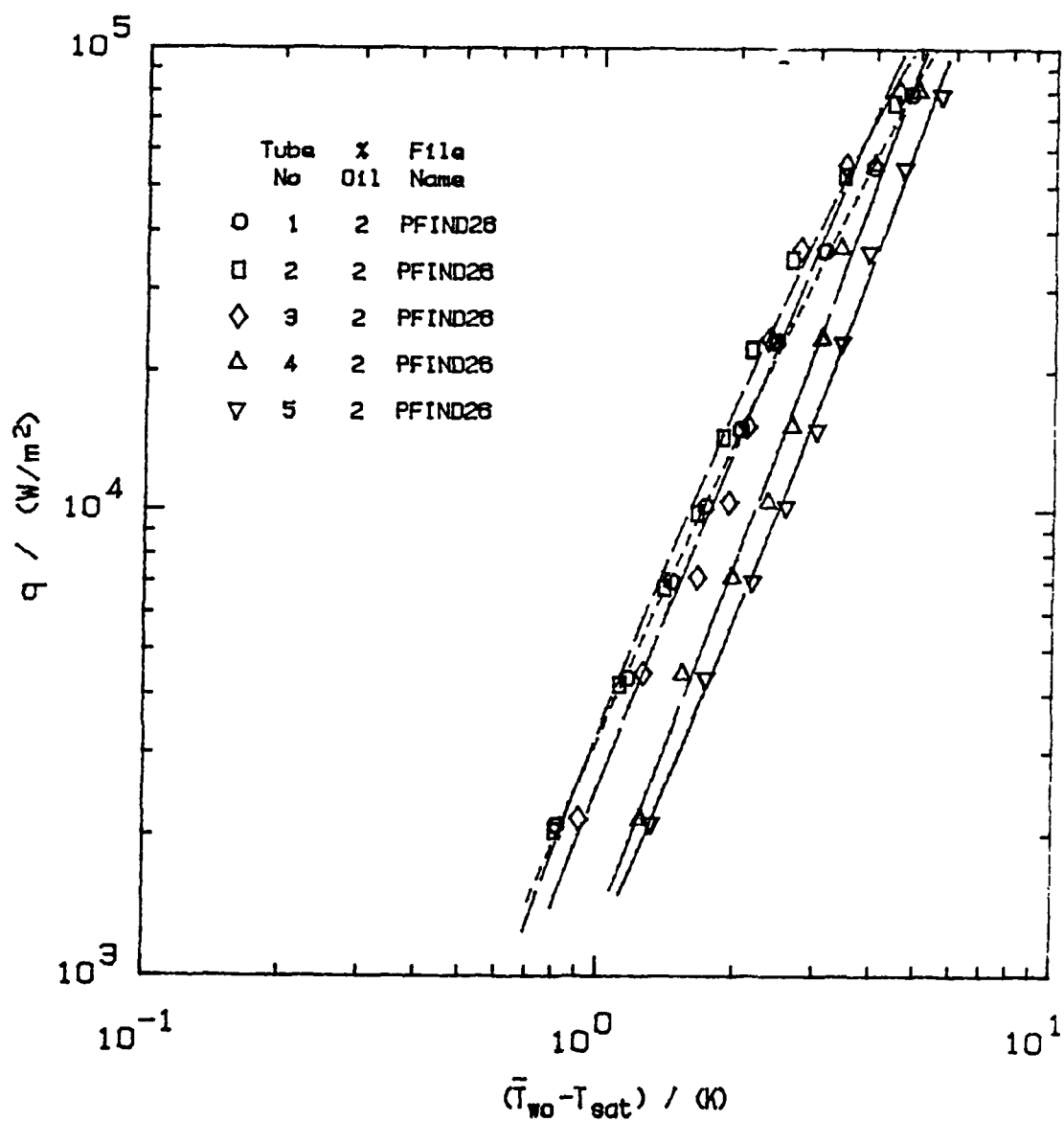


Figure 16. Heat Transfer Performance Results of Finned Tube Bundle with 2% Oil Concentration

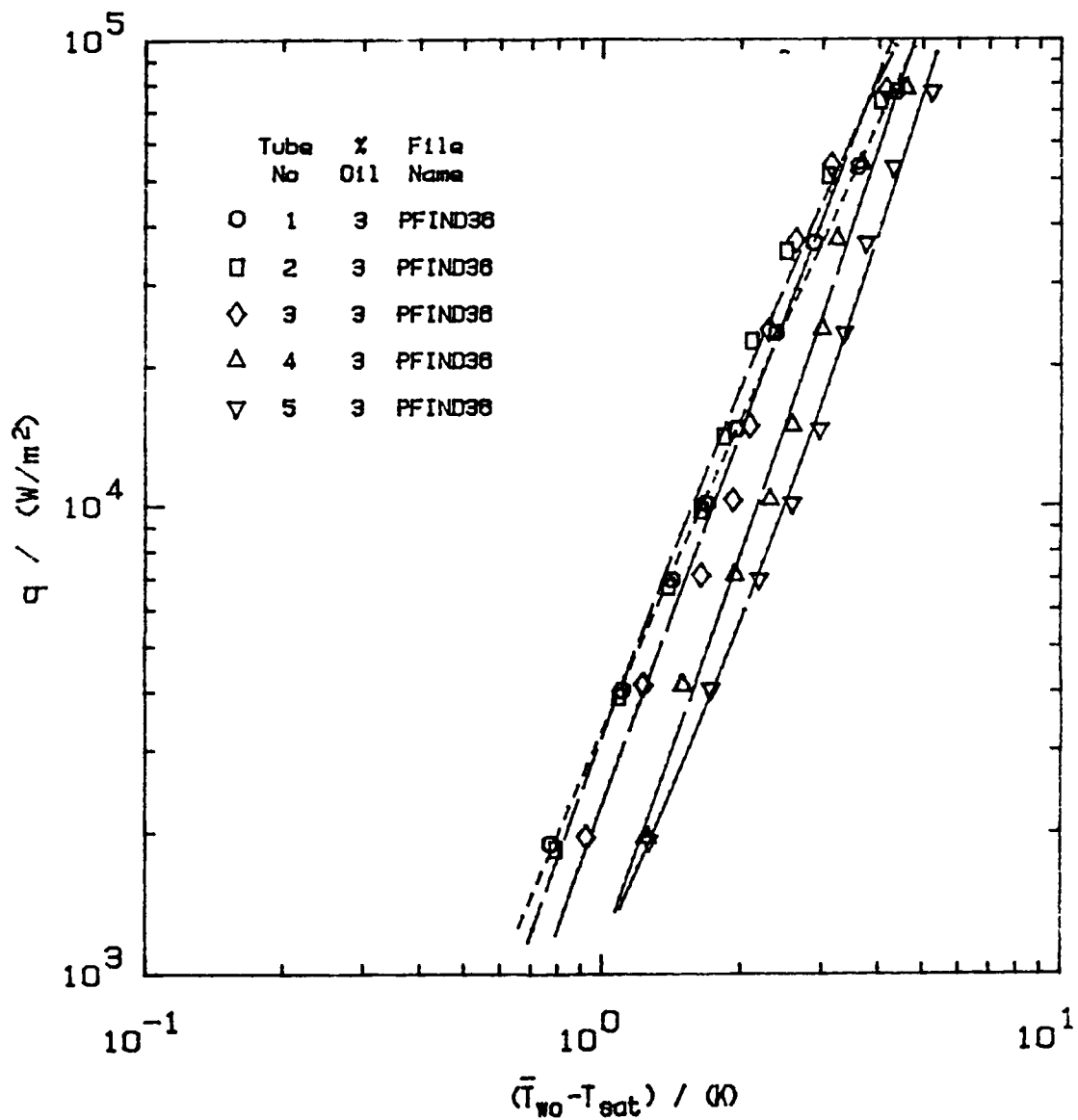


Figure 17. Heat Transfer Performance Results of Finned Tube Bundle with 3% Oil Concentration

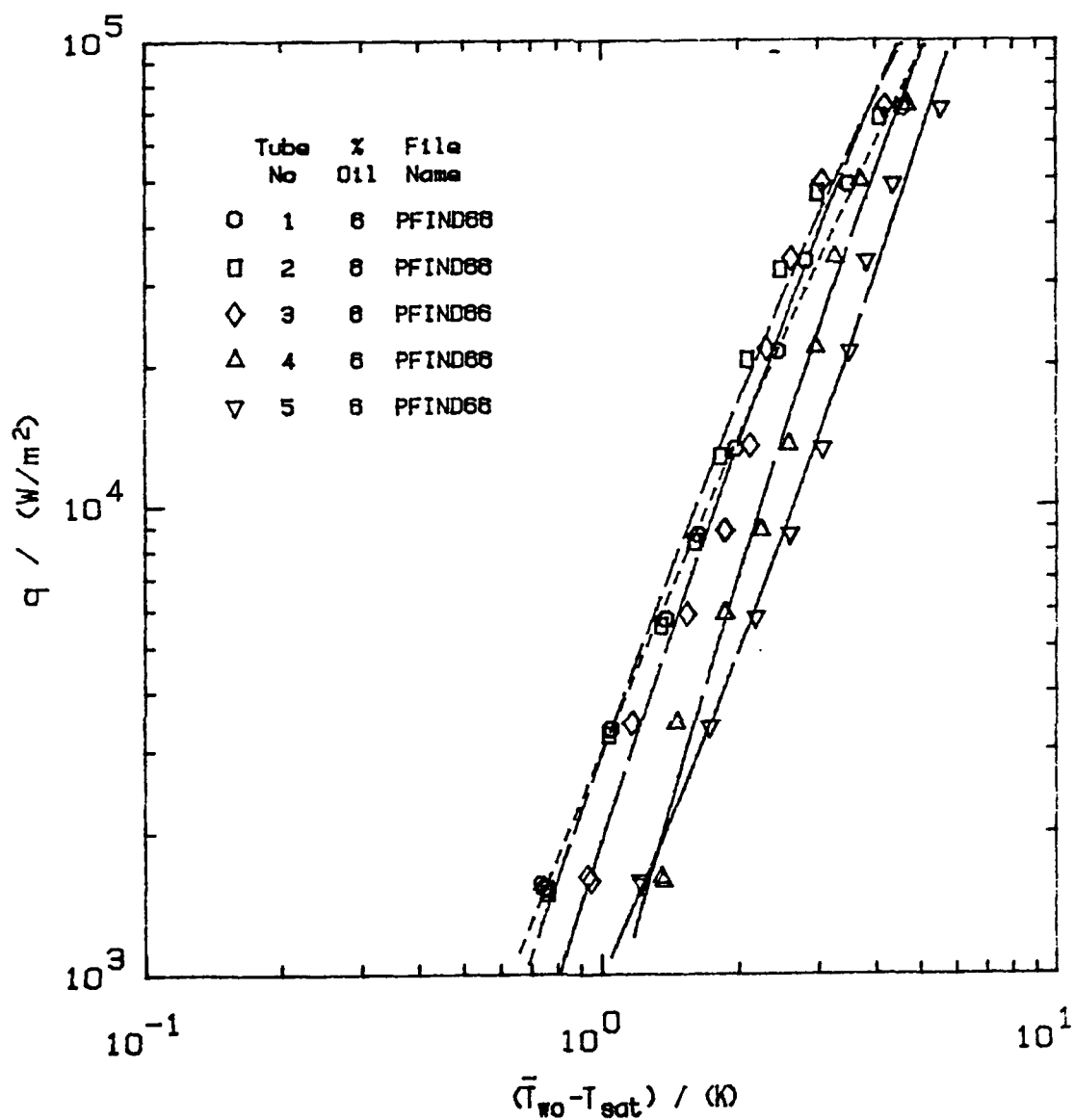


Figure 18. Heat Transfer Performance Results of Finned Tube Bundle with 6% Oil Concentration

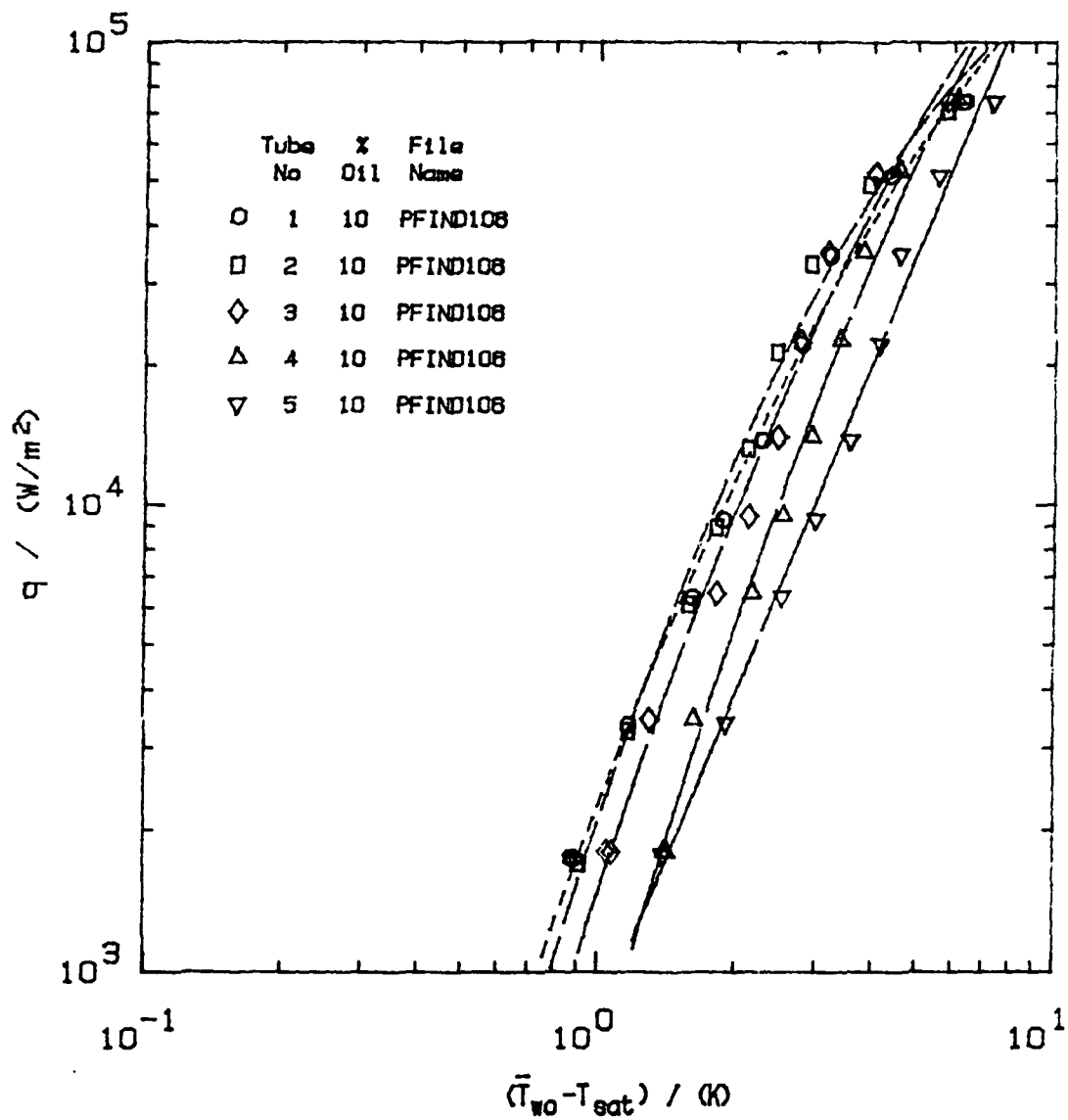


Figure 19. Heat Transfer Performance Results of Finned Tube Bundle with 10% Oil Concentration

D. R-114 BOILING FROM HIGH FLUX TUBE BUNDLE

Reilly [Ref. 18] tested the single High Flux tube performance in R-114 and R-114/Oil mixtures with a boiling temperature of -2.2 C. The result of his investigation for pure R-114 was plotted and compared to the result of this investigation. Figure 20 illustrates the variation of heat transfer coefficients with the heat flux. Reilly's result was better and the curves were nearly parallel along the entire heat flux range.

If the surface of the High Flux tubes is examined closely, the potential for a very high nucleation site density can be seen. These fine and dense nucleation sites cause numerous small bubbles. This high rate of bubble production creates a bubble coating around the tube surface. In bundle operation, bubbles produced from the lower tubes were not able to penetrate the upper tube bubble coating. Therefore, the convective effect of the rising bubbles was automatically eliminated. As a result, performance enhancement due to bundle operation was not noticeable for High Flux tubes. The conclusion given above can be observed in Figure 21. This figure shows the top tube (tube #1) performance variation with increasing number of heated tubes in the bundle. Almost the same curve was obtained from each different run. Consequently, the average bundle heat transfer performance approached the single tube performance since all instrumented tube performances remained nearly the same for different operations in the bundle. During bundle operation, the performance of tubes three and four seemed to diverge with increased heat flux. This behaviour can be related to increasing temperature differences between thermocouple readings on these tubes due to a nonhomogeneous distribution. Figure 22 displays the tube performances in the High Flux tube bundle. The effect of simulation heaters was negligible on the High Flux tube bundle performance and the bundle run with simulation heaters is shown in Figure 23.

E. R-114/OIL MIXTURE BOILING FROM HIGH FLUX TUBE BUNDLE

A single tube run was performed for each oil concentration and plotted. Figure 24 shows the performance variation of the top tube with various oil concentrations. With 1% oil addition, the performance response of the tube was immediately negative for all heat flux applications. Approximately 1 K increase was observed in the wall superheat. The performance curve stayed almost the same when 2% and 3% oil was added. The performance of the tube decreased significantly above a heat flux of 30 kW/m^2 with 6% oil and continued to decrease with 10% oil. There are not too many documented experimental results about the performance of High Flux tubes in R-114/Oil mixtures. Almost the same conclusions were obtained by Grant et al. [Ref. 15], from a single High

Flux tube in R-113/Oil mixtures. Wanniarachchi et al. [Ref 2] examined the High Flux tube performance in R-114/Oil mixtures and their results were parallel to the discussed results. Their discussion was valid about the degradation of High Flux tube performance with increased oil concentration. They indicated that a decrease in boiling performance at high heat fluxes and high oil concentrations may be a result of the creation an oil-rich layer within the boiling pores of the porous coating. The oil concentration within the pores must be larger than in the bulk liquid simply because from the mixture that migrates into the pores, where the actual boiling occurs, the R-114 liquid vaporizes leaving behind the oil. In this manner, the larger concentration of oil within the pores creates diffusion of oil back into the bulk mixture. At a steady-state condition, the mass of oil migrating into the pores with the bulk mixture balances the mass of oil diffusing back into the bulk. Therefore, the oil concentration within the pores is strongly dependent on the bulk oil concentration and the heat flux.

In bundle operation, all tubes showed a similar performance variation with oil concentration as mentioned for the top tube. The performance variation of the top tube can again be used as a representative of the average bundle performance variation under these circumstances. The High Flux tube bundle heat transfer coefficients for each oil addition and enhancement ratio are displayed in Table 7. Unlike for smooth and finned tubes, the presence of oil decreases the heat transfer performance of the High Flux tube. The fluctuation of produced bubbles was observed in High Flux tube bundle operations also. The frequency of fluctuation was higher than for the finned tube bundle due to higher flow circulation rate caused by a higher bubble production rate. It became more observable with increased oil concentration and no significant effects were obtained on performances due to this flow circulation. Figures 25 through 29 shows the performance variation of the High Flux tube bundle with variation of oil concentration.

F. PERFORMANCE COMPARISON OF THE FINNED, HIGH FLUX AND SMOOTH TUBE BUNDLES

Heat transfer coefficients of tube bundles were considered to be a function of a nucleate boiling component and a convective component. The convective effects on the smooth tube bundle were very large compared to nucleation effects at low heat flux levels. However the nucleation effects on the finned tube bundle were much higher than the smooth tube bundle at the same heat flux due to the fin cavities (ie. interfin spaces). The heat transfer process inside the cavity can not be easily influenced by outside convective effects. At higher heat fluxes, the heat transfer process was generally gov-

erned by nucleation in the finned tube bundle. Fujita et al. [Ref. 19] indicated that nucleation and convection effects each have their own area of influence for the High Flux tube type. If the nucleation site density is small, then the area available for convective effects will be large. Because of excellent nucleation characteristics of the porous surface, the nucleation site density will be very large and, hence, little area will be available for convective effects even at low heat fluxes.

The experimental results of the smooth, finned and High Flux tube bundles verify the preceding discussion. The performance of the single tubes was plotted in Figure 30. It is clear that the best performance curve was obtained from High Flux tube due to the benefit of nucleation. The finned tube performance was better than the smooth tube as expected. Figure 31 displays the performance variations of the top tubes during bundle operation in pure R-114. Notice that the bundle effect with the High Flux tube was negligible compared to the finned and smooth tubes. The average bundle heat transfer coefficients of each individual tube set were tabulated for various oil concentrations in Tables 5, 6 and 7. The chosen heat flux was 30 kW/m^2 . Even though the performance of the High Flux tube bundle decreased with increased oil concentration, it displayed better performance than the finned and smooth tube bundles up to a 10% oil mixture. However, when this particular heat flux was exceeded, the best performance was obtained from the finned tube bundle with 10% oil addition. Figure 32 gives this result showing the performance of High Flux, finned and smooth tube number one during bundle operation with 10% oil.

Table 5. BOILING HEAT TRANSFER COEFFICIENTS AND ENHANCEMENT RATIOS FOR SMOOTH TUBE BUNDLE AT A HEAT FLUX OF 30 KW/M²

% Oil	Bundle h (kW/m ² K)	Enhancement Ratio
0	2.59	1.00
1	3.21	1.24
2	3.72	1.44
3	3.60	1.39
6	3.19	1.23
10	2.57	0.99

Table 6. BOILING HEAT TRANSFER COEFFICIENTS AND ENHANCEMENT RATIOS FOR FINNED TUBE BUNDLE AT A HEAT FLUX OF 30 KW/M²

% Oil	Bundle h (kW/m ² K)	Enhancement Ratio
0	6.56	1.00
1	8.31	1.27
2	10.38	1.58
3	10.80	1.65
6	10.52	1.60
10	9.03	1.38

Table 7. BOILING HEAT TRANSFER COEFFICIENTS AND ENHANCEMENT RATIOS FOR HIGH FLUX TUBE BUNDLE AT A HEAT FLUX OF 30 KW/M²

% Oil	Bundle h (kW/m ² K)	Enhancement Ratio
0	16.61	1.00
1	14.17	0.85
2	14.40	0.87
3	14.50	0.87
6	13.72	0.82
10	8.75	0.53

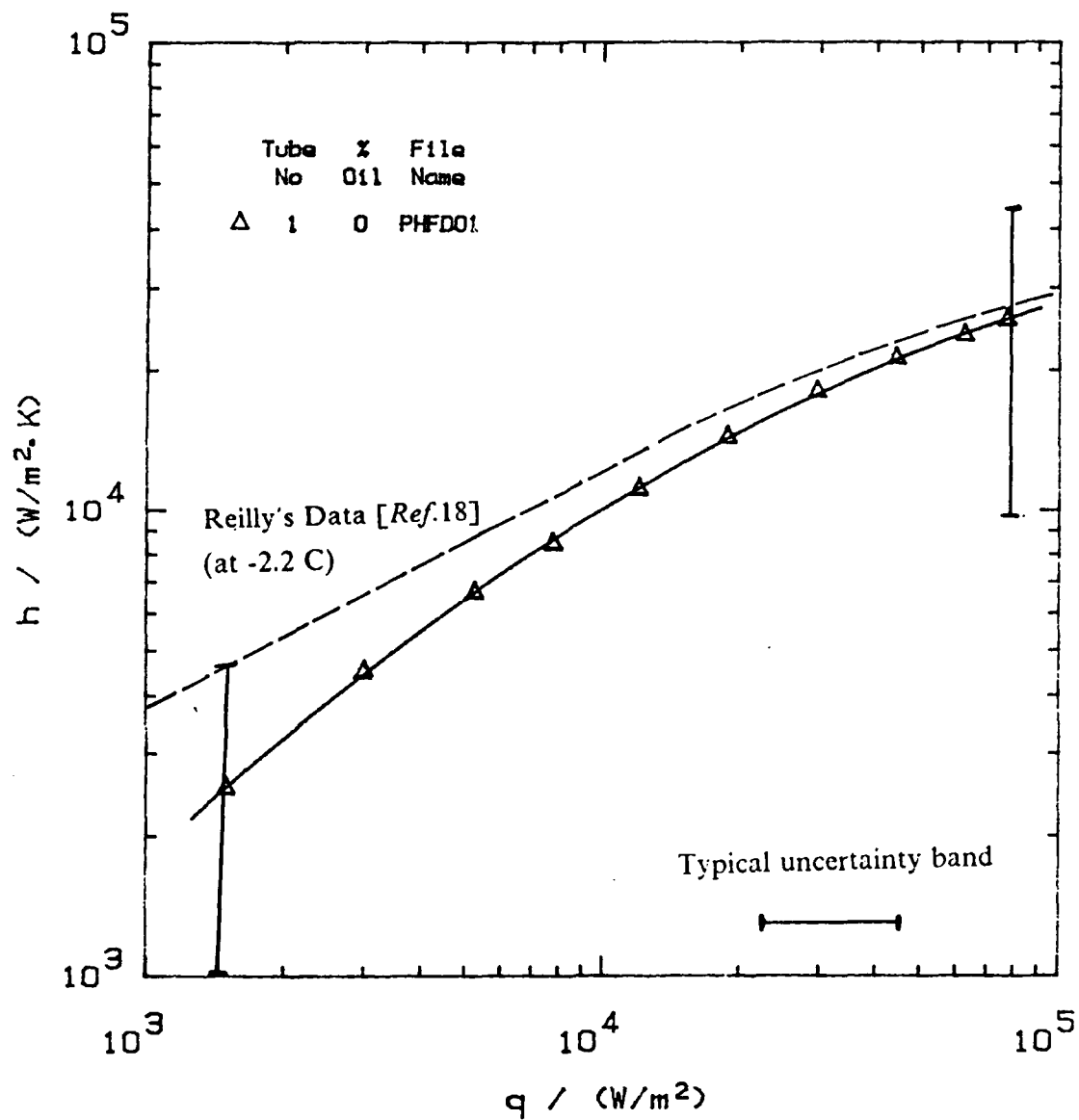


Figure 20. Single High Flux Tube Performance in Pure R-114 within High Flux Tube Bundle

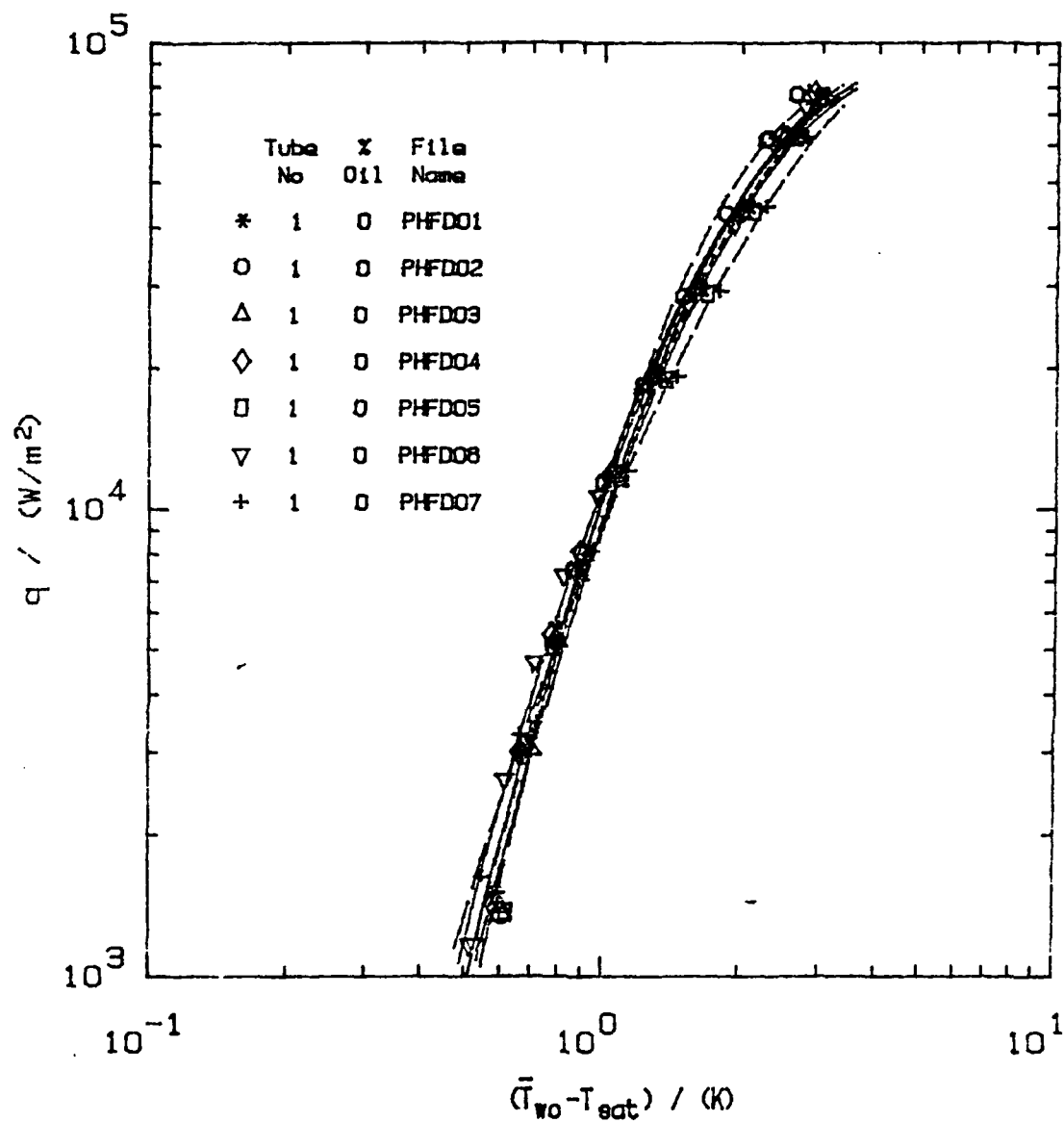


Figure 21. Performance Variation of Tube Number one in R-114 when Influenced by Increasing Number of Heated Tubes in H. Flux Tube Bundle

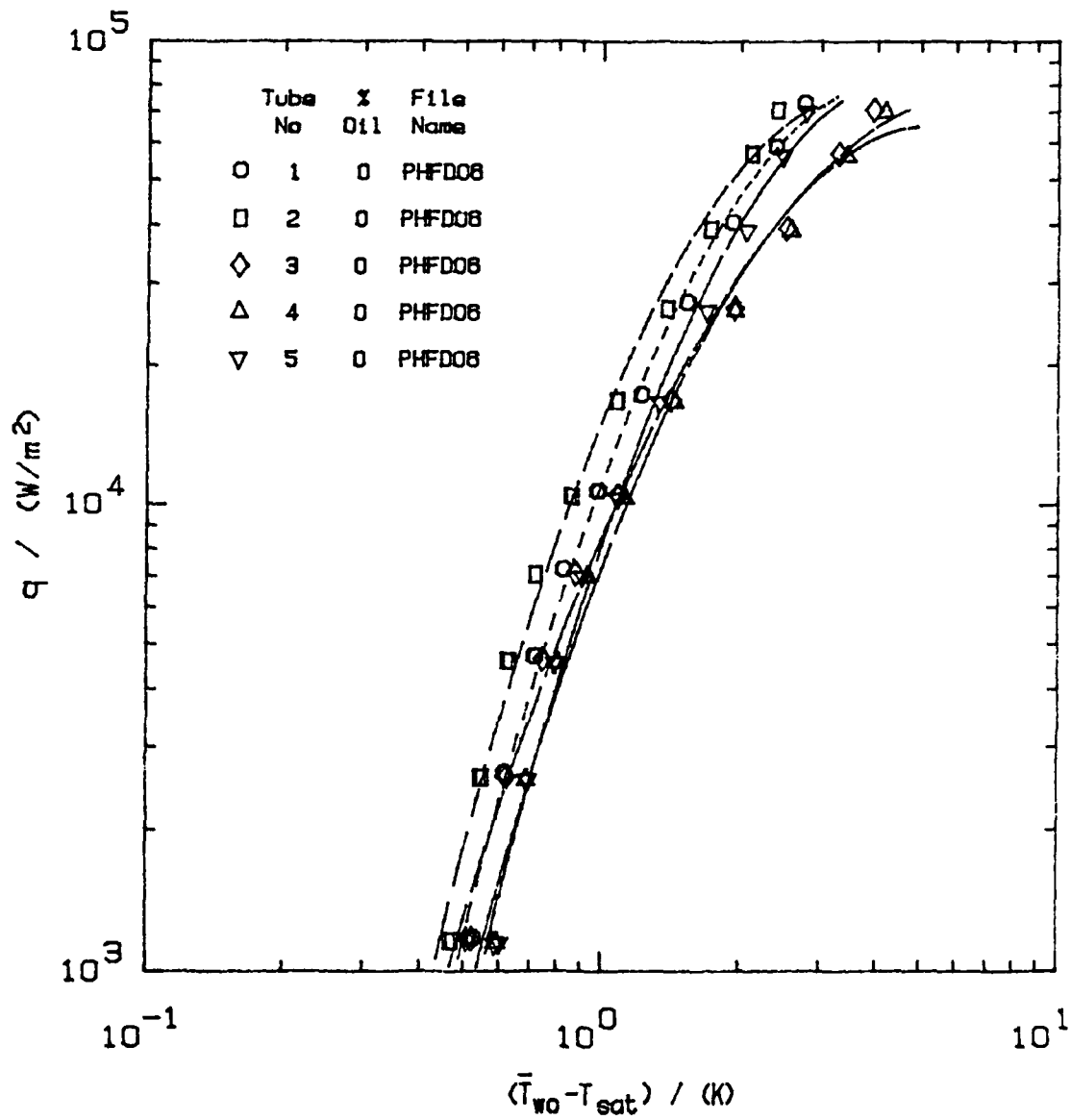


Figure 22. Heat Transfer Performance Results of High Flux Tube Bundle in Pure R-114

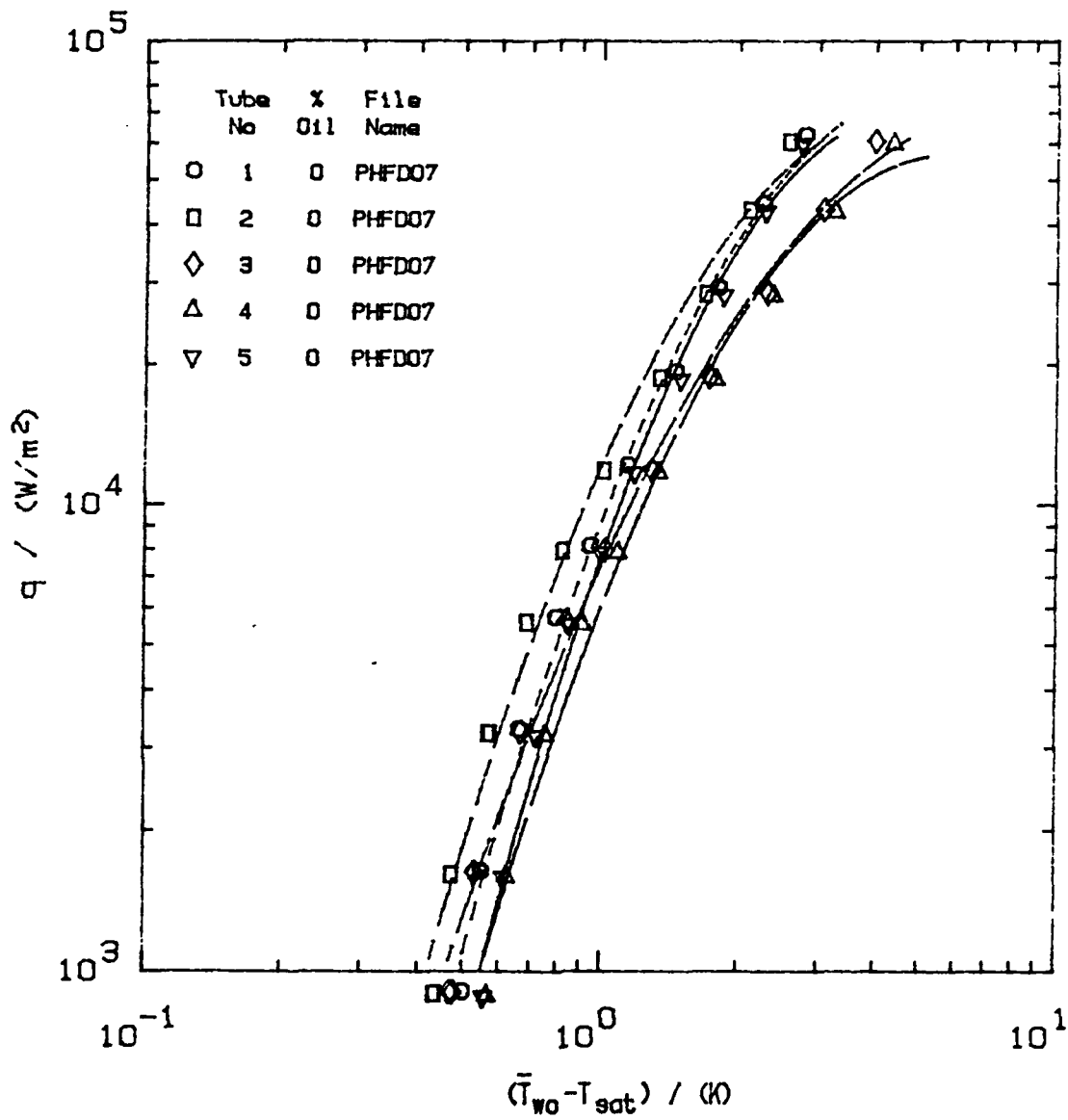


Figure 23. Heat Transfer Performance Results of High Flux Tube Bundle with Simulation Heaters in Pure R-114

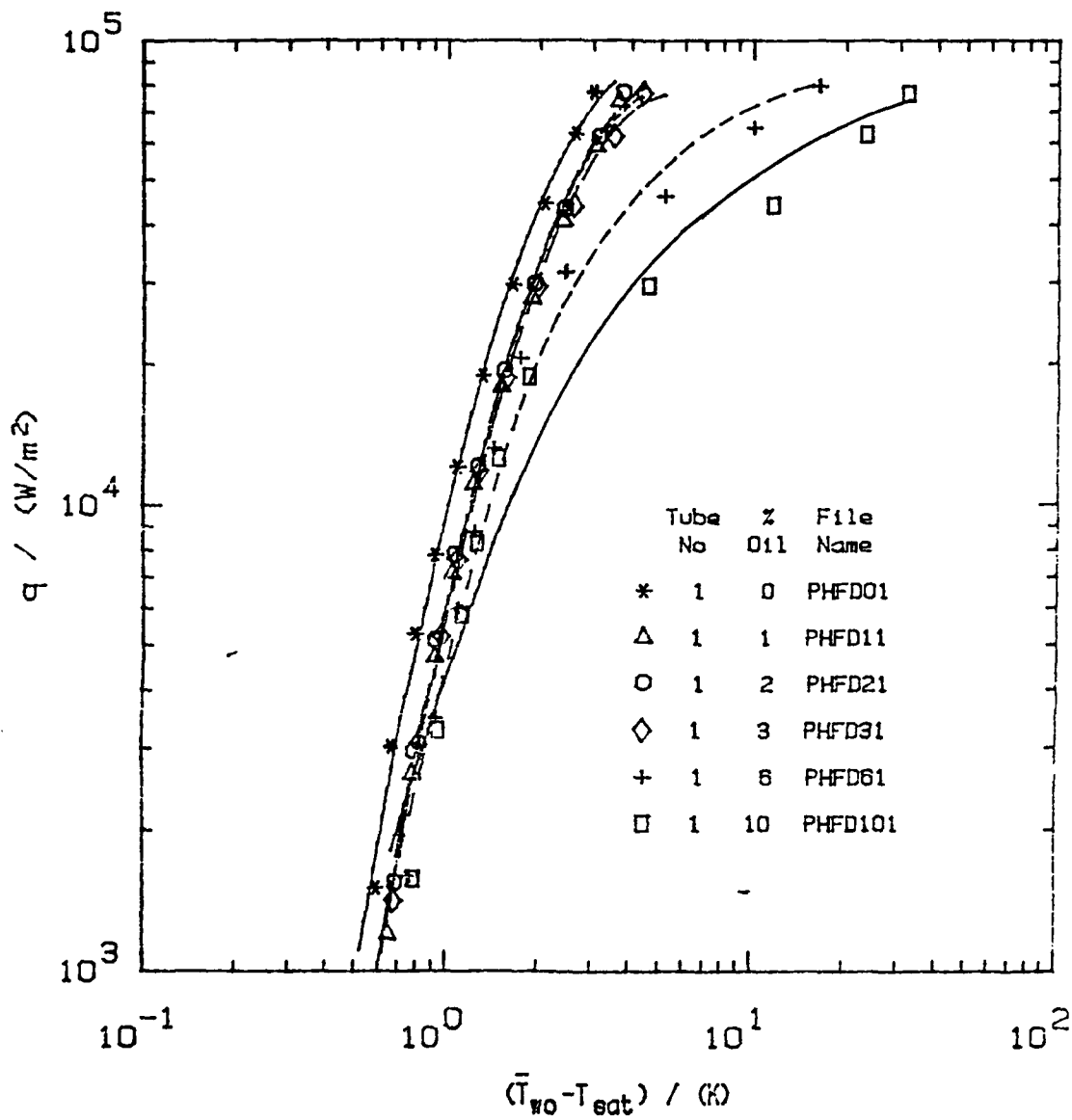


Figure 24. Performance Variation of Tube Number One with Variation of Oil Concentration in High Flux Tube Bundle

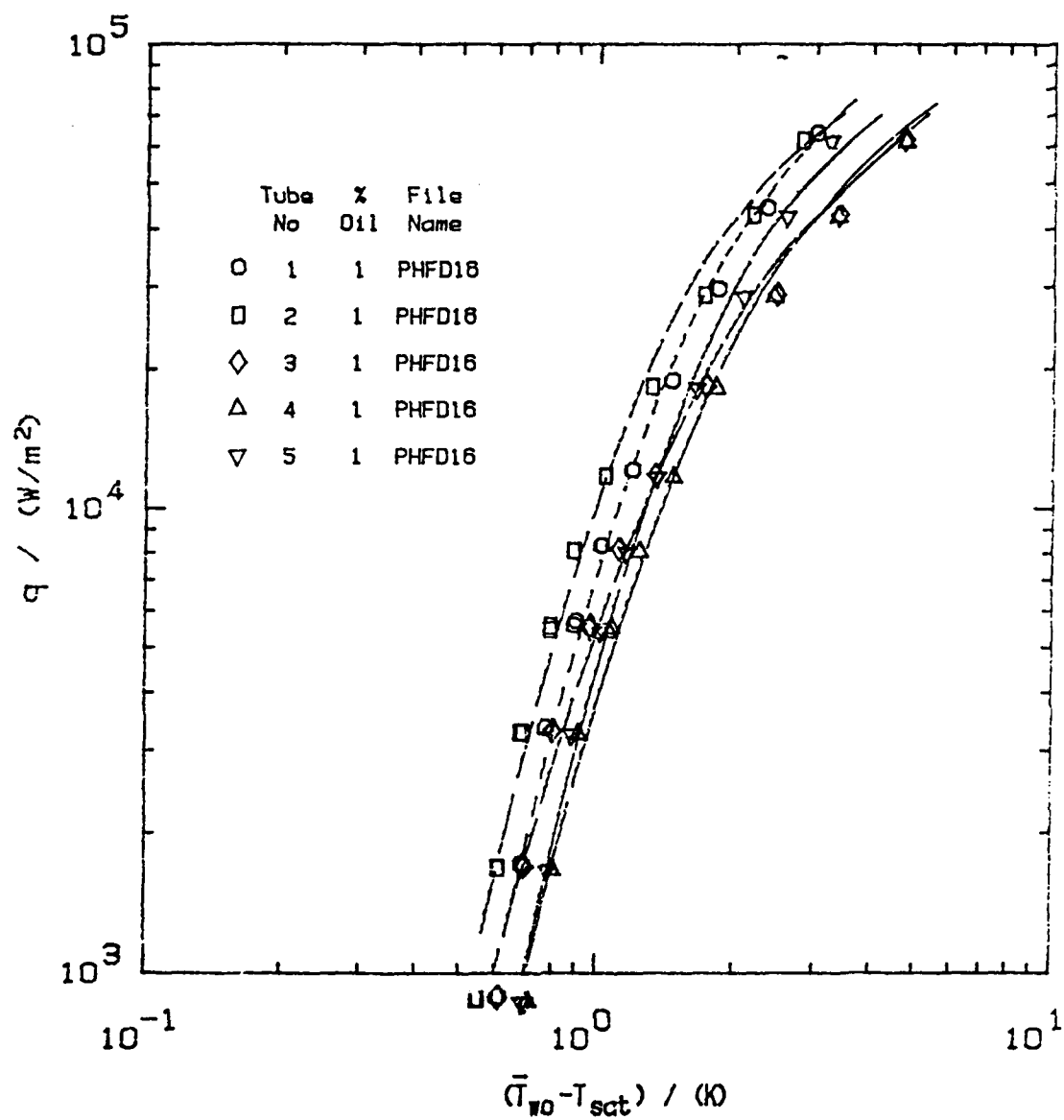


Figure 25. Heat Transfer Performance Results of High Flux Tube Bundle with 1% Oil Concentration

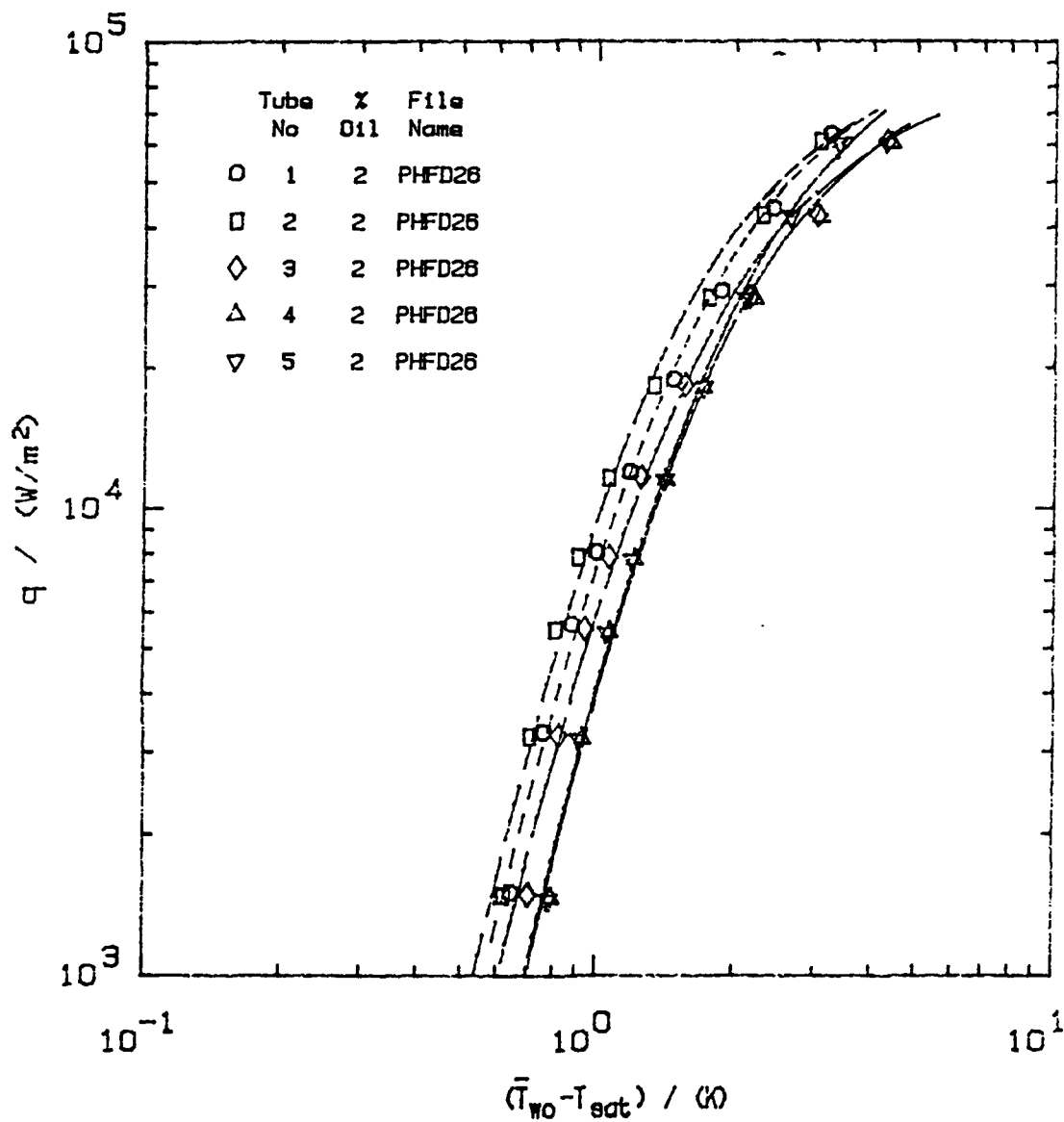


Figure 26. Heat Transfer Performance Results of High Flux Tube Bundle with 2% Oil Concentration

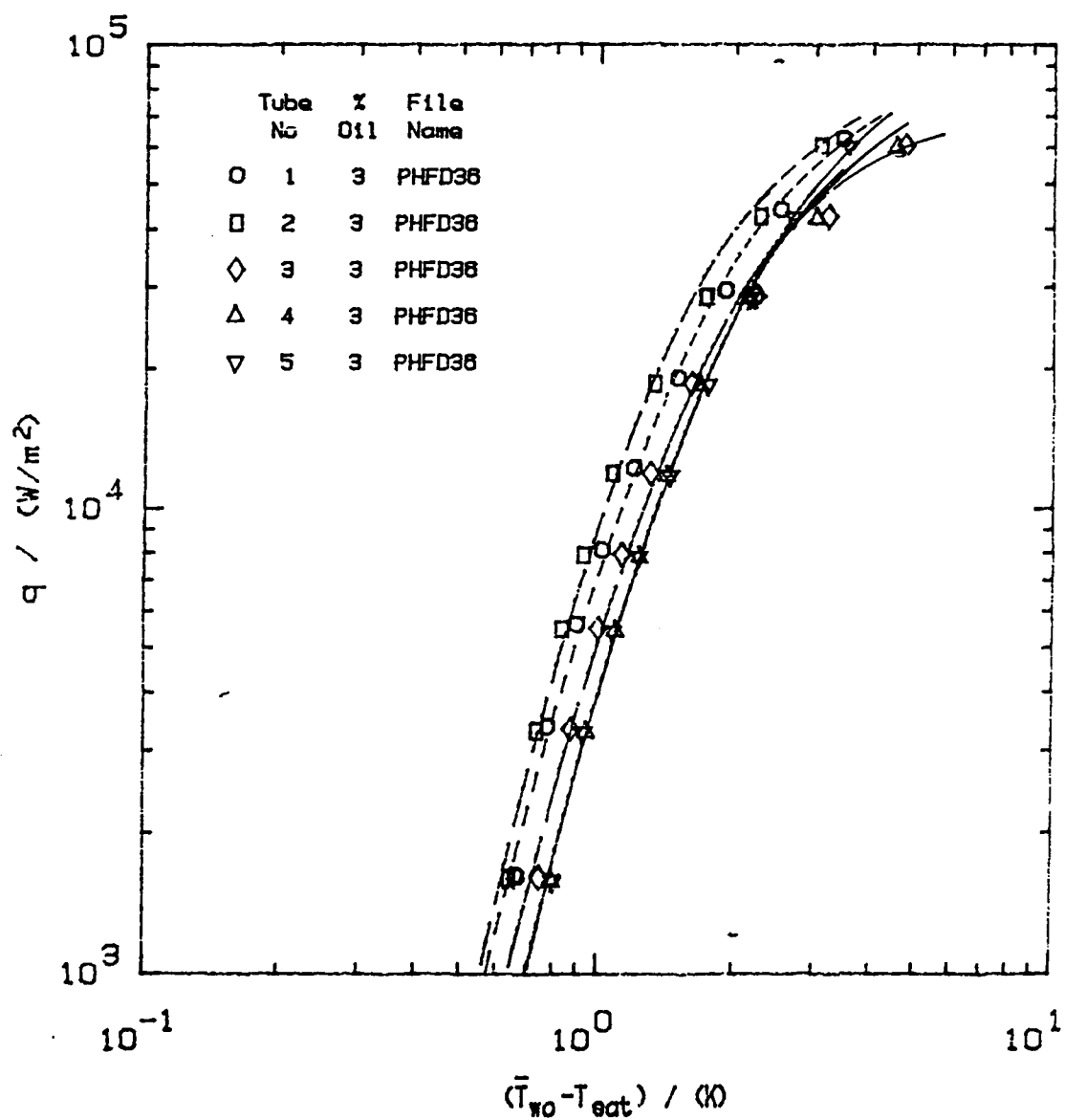


Figure 27. Heat Transfer Performance Results of High Flux Tube Bundle with 3% Oil Concentration

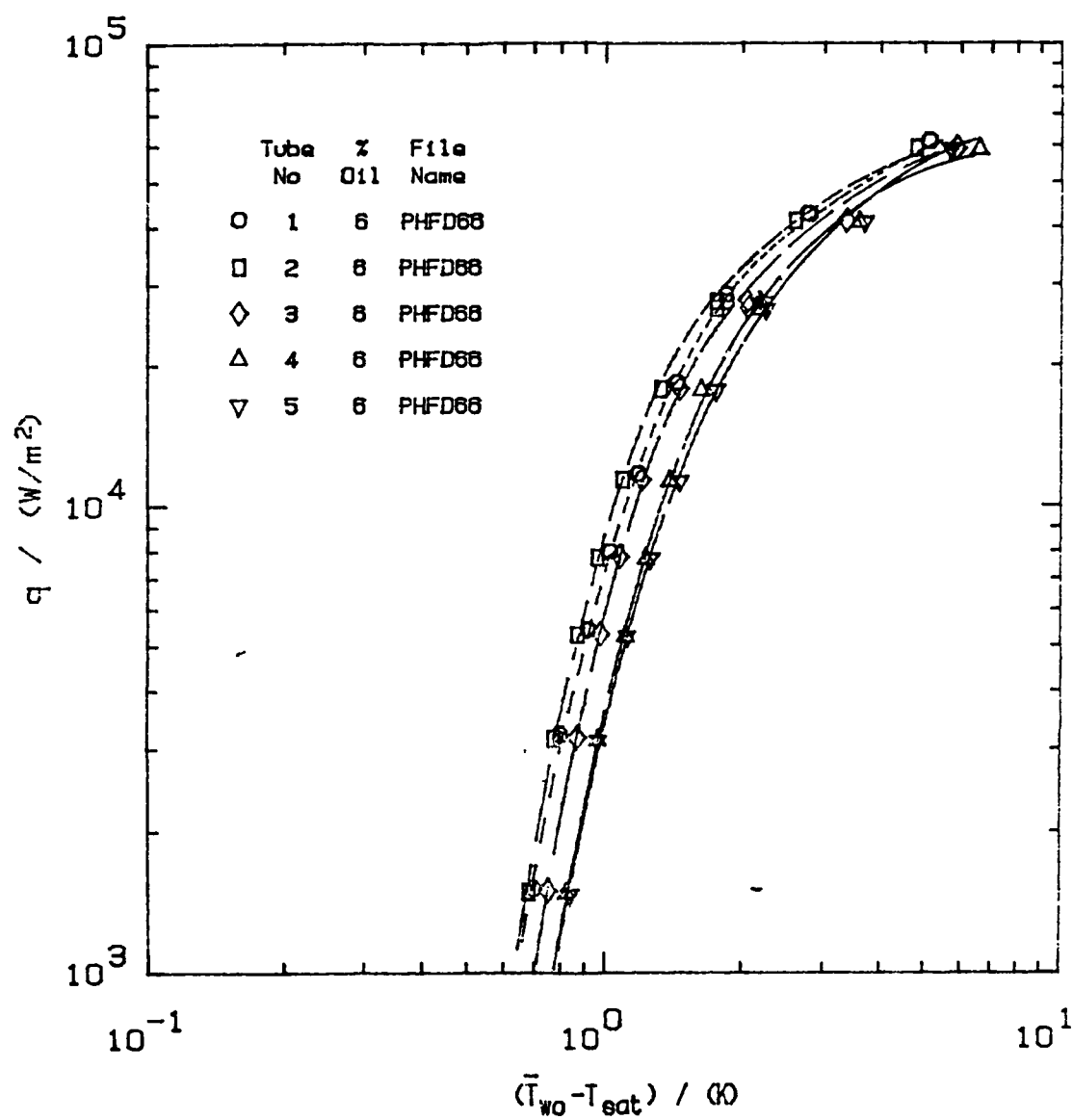


Figure 28. Heat Transfer Performance Results of High Flux Tube Bundle with 6% Oil Concentration

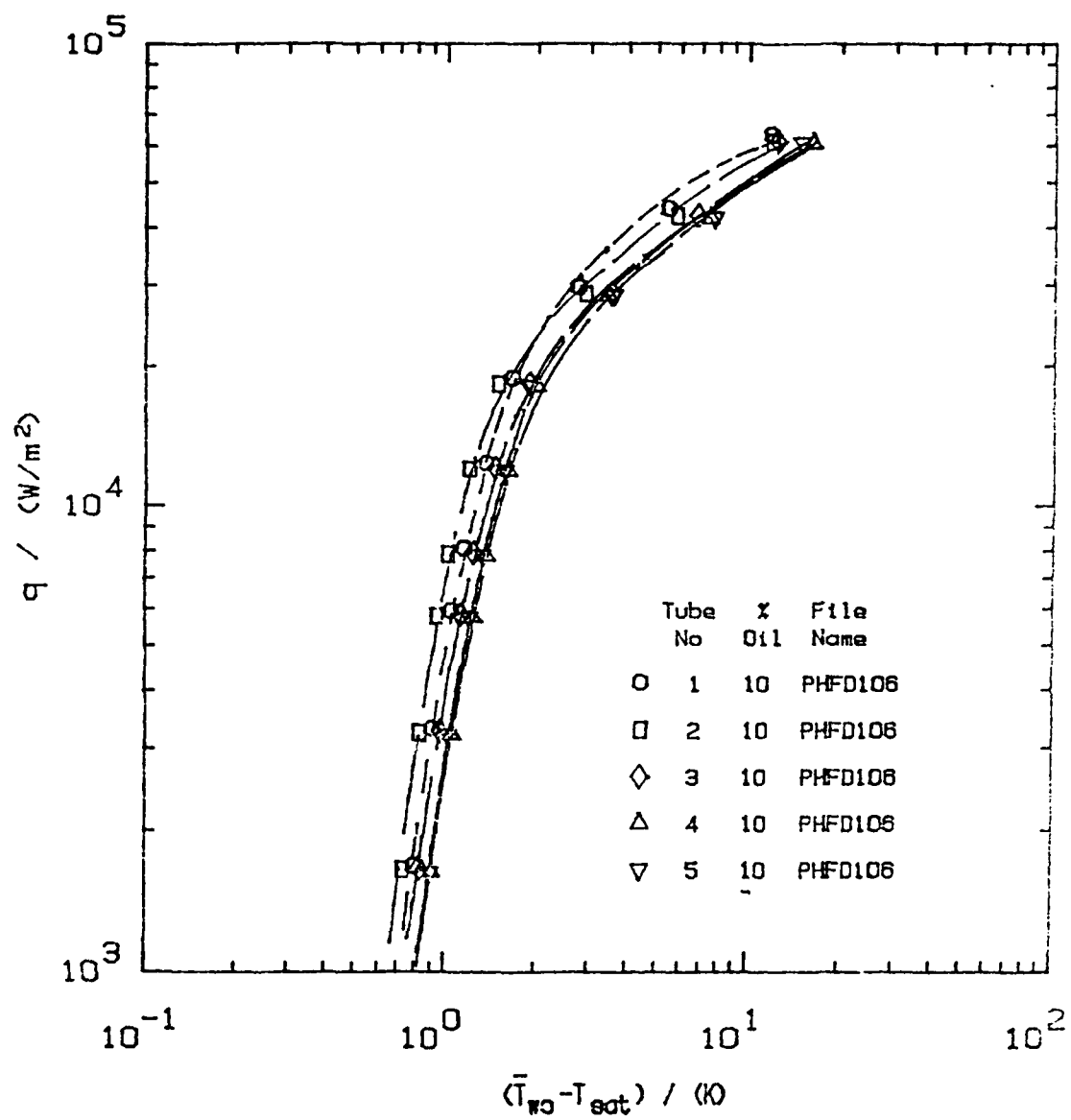


Figure 29. Heat Transfer Performance Results of High Flux Tube Bundle with 10% Oil Concentration

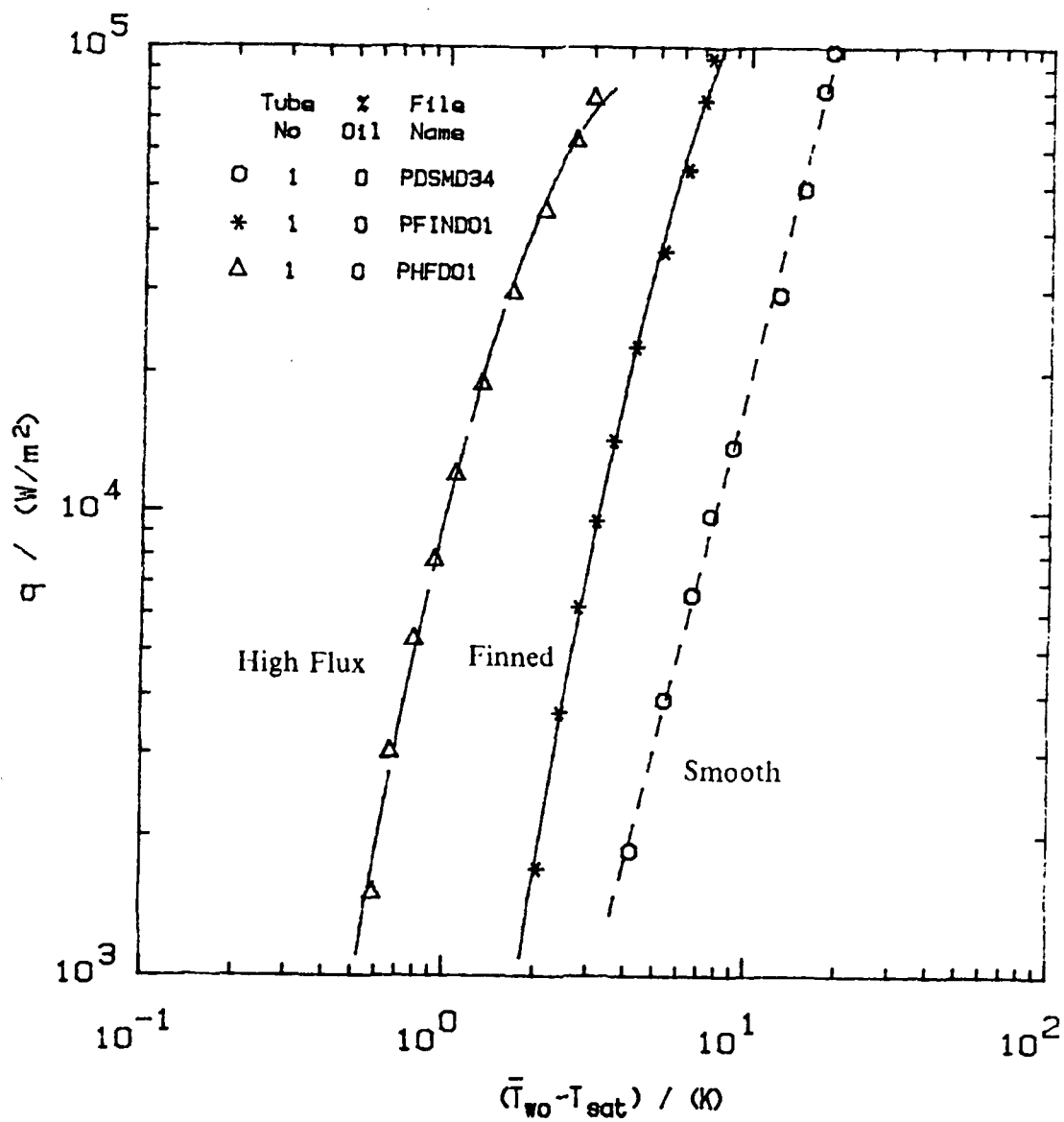


Figure 30. Comparison of High Flux, Finned and Smooth Single Tube Performances in Pure R-114

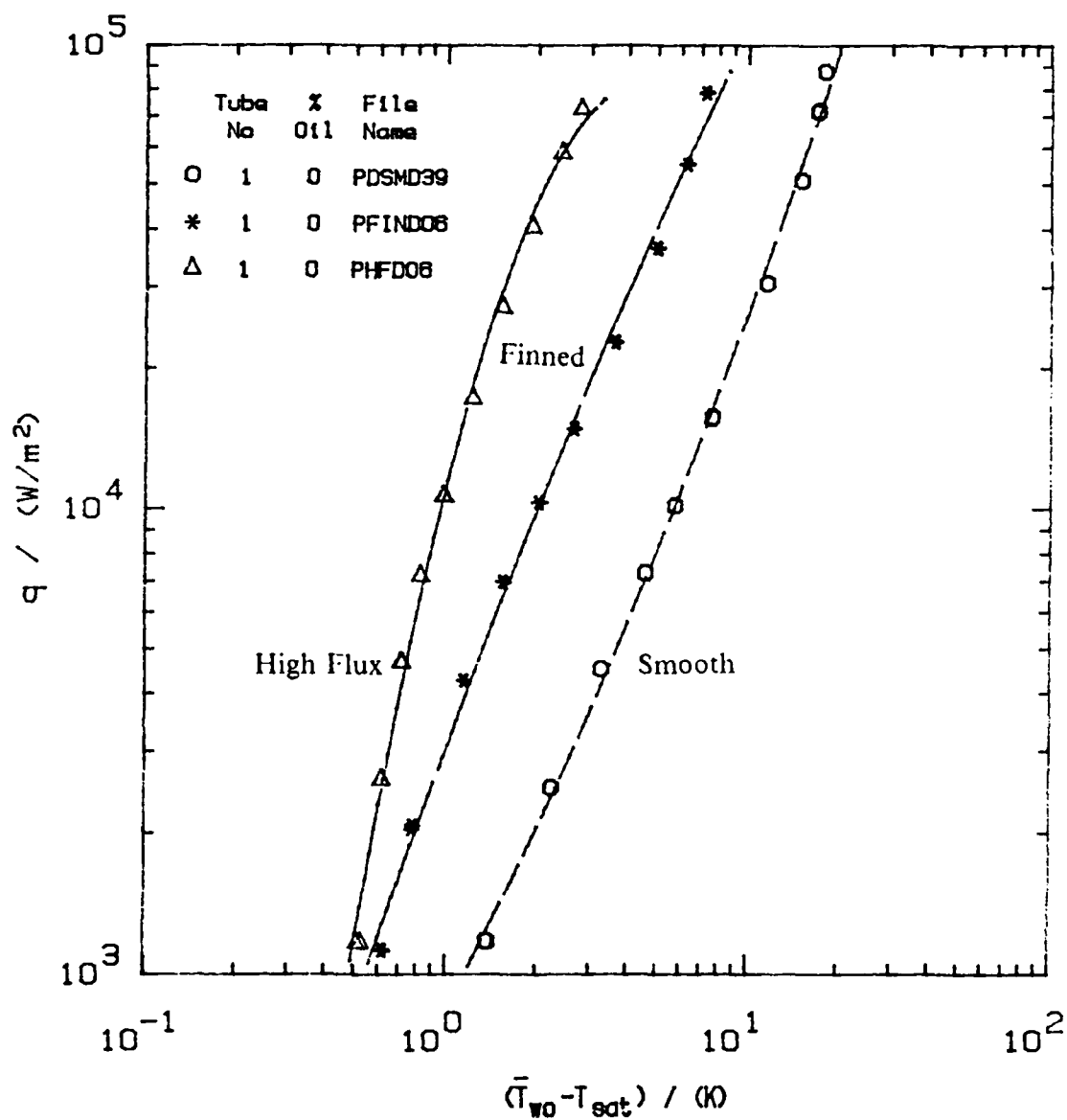


Figure 31. Comparison of High Flux, Finned and Smooth Top Tube Performances during Bundle Operation in Pure R-114

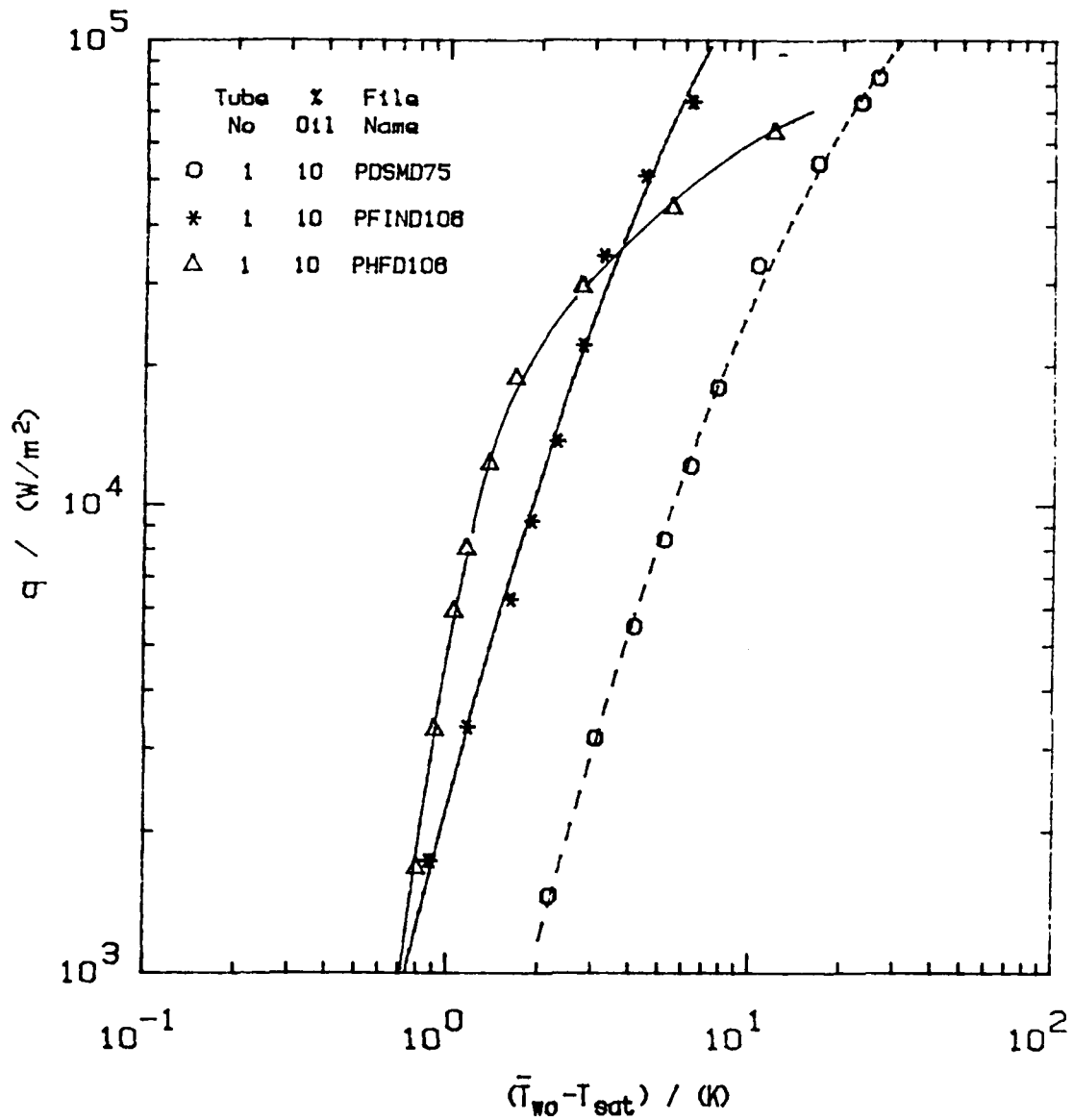


Figure 32. Comparison of High Flux, Finned and Smooth Top Tube Performances during Bundle Operation with 10% Oil concentration

VI. CONCLUSIONS AND RECOMMENDATIONS

A. CONCLUSIONS

The finned and High Flux tube bundles were tested during boiling in R-114 and R-114/Oil mixtures. Considering the obtained heat transfer results of each type of tube set, the following conclusions were reached.

1. The performance of the finned tube bundle was determined to be approximately twice as good as the single tube. This is a result of a positive bundle effect.

2. Oil addition affected the finned tube bundle performance positively, particularly at high heat fluxes. Bundle performance increased 2.5 times with 3% oil contamination compared to pure R-114 at the maximum heat flux level. At low heat flux applications, the positive effect is diminished. For 6% and 10% oil concentrations, the performance of bundle was decreased slightly below the pure R-114 condition.

3. Each individual High Flux tube performance was not affected by increasing the number of heated tubes in the bundle. The bundle effect for the High Flux tube was negligible, therefore the bundle performance approached the single tube performance.

4. The effectiveness of the High Flux tube bundle degraded with increased amount of oil. The degradation was significant at a high heat flux and with 6% and 10% oil concentrations. At a heat flux of 30 kW/m^2 28% and 47% degradation from pure R-114 was observed for 6% and 10% oil concentrations respectively.

5. The best bundle performance was obtained from the High Flux tubes. It was 6.4 and 2.5 times better than the smooth tube and the finned tube bundle performances at a heat flux of 30 kW/m^2 , respectively (in pure R-114). These performance ratios decreased with increased oil concentrations. Above a heat flux of 30 kW/m^2 , the performance of the finned tube bundle became better in 6% or greater oil concentrations.

B. RECOMMENDATIONS

1. The tube fabrication technique should be examined more fully in order to get a more uniform temperature distribution along the tube wall.
2. The temperature distribution along the cartridge heater should be determined and a nonuniform temperature distribution should be accounted for.
3. The fourth thermocouple on the tube number four displayed a defective reading (Channel 62) for each tube set run. There are 30 total thermocouples on the instrumented tubes. With this in mind, the possibility of defectiveness from a thermocouple itself can be highly reduced. Therefore, the junction of thermocouple wires up to the data reduction unit and the channel number 62 should be checked.
4. The method for oil addition should be improved in order to facilitate easier, more accurate and safer oil addition to the freon.
5. The data reduction program "DRP4" can be modified to alert the operator when the critical heat flux for freon decomposition is exceeded. This will help eliminate operator faults.
6. The observed bubble fluctuations at high heat fluxes during bundle operation should be examined and compared with real applications.
7. The negative effects of oil at low heat fluxes for the finned tube bundle operation should be investigated and the reasons should be clarified.
8. The air circulation in the experiment room should be increased to eliminate the negative effect of freon vapor to the human body.

APPENDIX A. LISTING OF DATA FILES

Table 8. DATA FILE NAMES OF THE FINNED AND HIGH FLUX TUBE RUNS

File Name (Finned)	File Name (H. Flux)	Number of Data Points	Number of Heated tubes	Percent Oil	Number of Ac- tive Pairs	Number of Sim- ulated Tubes
FIND01	HFD01	20	1	0	0	0
FIND02	HFD02	20	2	0	0	0
FIND03	HFD03	20	3	0	0	0
FIND04	HFD04	20	4	0	0	0
FIND05	HFD05	20	5	0	0	0
FIND06	HFD06	20	5	0	5	0
FIND07	HFD07	20	5	0	5	5
FIND11	HFD11	20	1	1	0	0
FIND12	HFD12	20	2	1	0	0
FIND13	HFD13	20	3	1	0	0
FIND14	HFD14	20	4	1	0	0
FIND15	HFD15	20	5	1	0	0
FIND16	HFD16	18/20	5	1	5	0
FIND17	HFD17	18	5	1	5	5
FIND21	HFD21	20	1	2	0	0
FIND22	HFD22	20	2	2	0	0
FIND23	HFD23	20	3	2	0	0
FIND24	HFD24	20	4	2	0	0
FIND25	HFD25	20	5	2	0	0
FIND26	HFD26	18	5	2	5	0
FIND27	HFD27	18	5	2	5	5
FIND31	HFD31	20	1	3	0	0
FIND32	HFD32	20	2	3	0	0
FIND33	HFD33	20	3	3	0	0
FIND34	HFD34	20	4	3	0	0
FIND35	HFD35	20	5	3	0	0
FIND36	HFD36	18	5	3	5	0

Table 8(contd.). DATA FILE NAMES OF FINNED AND HIGH FLUX TUBE RUNS

FIND37	HFD37	18	5	3	5	5
FIND61	HFD61	20	1	6	0	0
FIND62	HFD62	20	2	6	0	0
FIND63	HFD63	20	3	6	0	0
FIND64	HFD64	20	4	6	0	0
FIND65	HFD65	20	5	6	0	0
FIND66	HFD66	18	5	6	5	0
FIND67	HFD67	18	5	6	5	5
FIND101	HFD101	20	1	10	0	0
FIND102	HFD102	20	2	10	0	0
FIND103	HFD103	20	3	10	0	0
FIND104	HFD104	20	4	10	0	0
FIND105	HFD105	20	5	10	0	0
FIND106	HFD106	18	5	10	5	0
FIND107	HFD107	18	5	10	5	5

APPENDIX B. SAMPLE CALCULATIONS

A test file was created and the data of tube number two from the High Flux tube bundle was used for sample calculations and program validation.

1. Test tube dimensions

$$D_o = 15.8 \text{ mm}$$

$$D_i = 11.6 \text{ mm}$$

$$D_{ic} = 10.6 \text{ mm}$$

$$L = 203.2 \text{ mm}$$

$$L_u = 25.4 \text{ mm}$$

2. Measured parameters

$$T1 = 3.90 \text{ C}$$

$$T2 = 3.69 \text{ C}$$

$$T3 = 3.99 \text{ C}$$

$$T4 = 4.37 \text{ C}$$

$$T5 = 4.29 \text{ C}$$

$$T6 = 4.10 \text{ C}$$

$$T1d1 = 2.16 \text{ C}$$

$$T1d2 = 2.19 \text{ C}$$

$$Aas = 2.24 \text{ V}$$

$$Vas = 2.11 \text{ V}$$

3. Calculations

The heater power is calculated as

$$q = Vas \times Aas \times 60 \times 1 \quad (B.1)$$

The multiplication factors of the volt and amp sensors are 60 and 1 respectively, then

$$q = 2.11 \times 2.24 \times 60 \times 1$$

$$q = 283.58 \text{ W}$$

The tube inside wall temperature is obtained from the average value of six thermocouple readings.

$$\bar{T}_{wl} = \frac{1}{6} \times \sum_{n=1}^6 T_n \quad (B.2)$$

$$\bar{T}_{wl} = \frac{1}{6} \times (3.90 + 3.69 + 3.99 + 4.37 + 4.29 + 4.10)$$

$$\bar{T}_{wl} = 4.06 \text{ C}$$

The tube outside temperature is calculated using Fourier's conduction term and the tube inside wall temperature. Uniform radial conduction is assumed in the tube wall.

$$\bar{T}_{wo} = \bar{T}_{wl} - \frac{q \times \ln\left(\frac{D_o}{D_{ic}}\right)}{2 \times \pi \times k_{cu} \times L} \quad (B.3)$$

where k_{cu} is thermal conductivity and is calculated at \bar{T}_{wl} as follows

$$k_{cu} = 434.0 - (0.112 \times \bar{T}_{wl-K}) \quad (B.4)$$

$$k_{cu} = 434.0 - (0.112 \times 277.21)$$

$$k_{cu} = 402.95 \frac{W}{m \text{ K}}$$

now,

$$\bar{T}_{wo} = 4.06 - \frac{283.58 \times \ln\left(\frac{15.8}{10.6}\right)}{2 \times \pi \times 402.95 \times 0.2032}$$

$$\bar{T}_{wo} = 3.84 \text{ C}$$

The liquid saturation temperature at the top of the tube bank is

$$T_{sat} = \frac{T_{ld1} + T_{ld2}}{2} \quad (B.5)$$

$$T_{sat} = \frac{2.16 + 2.19}{2}$$

$$T_{sat} = 2.175 \text{ C}$$

In order to calculate the local saturation temperature for each tube, small corrections are needed due to the hydrostatic pressure difference between the tube location and liquid free surface. This difference is calculated for tube two by

$$\Delta P = \rho \times g \times h_t \quad (B.6)$$

$$\Delta P = 1521.47 \times 9.81 \times 0.0452$$

$$\Delta P = 674.64 \text{ Pa}$$

For 674.64 Pa pressure difference correct saturation temperature is found by adding 0.181 C (from standart tables for R-114) to T_{sat} . It becomes

$$T_{sat} = 2.175 + 0.181 \quad (B.7)$$

$$T_{sat} = 2.36 \text{ C}$$

and the wall superheat becomes

$$\Delta T = \bar{T}_{wo} - T_{sat} \quad (B.8)$$

$$\Delta T = 3.84 - 2.36$$

$$\Delta T = 1.48 \text{ C}$$

The test tube is 12 inches long and only the middle section of 8 inches is uniformly heated leaving a 1-inch and 3-inch long unheated section at either end. The 1 and 3 inch unheated lengths behave as fins in the heat transfer process. The following procedure is applied to the unheated ends of the tubes. Calculations are shown for the one inch length only.

Heat transferred from the unheated end is calculated as heat from the base of a fin:

$$q_f = (h_b \times p \times k_{cu} \times A_s)^{0.5} \times \Delta T \times \tanh(n \times L_c) \quad (B.9)$$

where

$$p = \pi \times D_o \quad (B.10)$$

$$p = 49.64 \times 10^{-3} \text{ m}$$

and

$$A_c = \frac{\pi}{4} \times (D_o^2 - D_i^2) \quad (B.11)$$

$$A_c = \frac{\pi}{4} \times (0.0158^2 - 0.0116^2)$$

$$A_c = 90.38 \times 10^{-6} m^2$$

The corrected length of unenhanced surface at the end can be calculated as

$$L_c = L_u + \frac{l}{2} \quad (B.12)$$

$$L_c = 0.0254 + \frac{(0.0158 - 0.0116)}{4}$$

$$L_c = 0.0264 m$$

$$n = \left(\frac{h_b \times p}{k_{cu} \times A_c} \right)^{0.5} \quad (B.13)$$

h_b is the natural convection heat transfer coefficient of the finned-like ends and can be calculated using Churchill-Chu [Ref. 20] correlation for natural convection from a smooth horizontal cylinder, which was modified by Pulido [Ref. 21].

$$h_b = \frac{k}{D_o} \times \left\{ .6 + .387 \times \frac{\left(\frac{g \times \beta \times D_o^3 \times \Delta T \times \tanh(n \times L_c)}{\nu \times \alpha \times L_c \times n} \right)^{\frac{1}{6}}}{\left[1 + \left(\frac{0.559}{Pr} \right)^{\frac{9}{16}} \right]^{\frac{8}{27}}} \right\}^2 \quad (B.14)$$

An iteration technique is necessary to calculate h_b . The physical properties are calculated at the vapor mean film temperature which is

$$T_{film} = \frac{T_{sat} + \bar{T}_{wo}}{2} \quad (B.15)$$

$$T_{film} = \frac{2.175 + 3.84}{2}$$

$$T_{film} = 3.008 C$$

or

$$T_{film_K} = 276.16 \text{ K}$$

then for R-114

$$\mu = \exp\left[-4.4636 + \left(\frac{1011.47}{T_{film_K}}\right)\right] \times 10^{-3} \quad (B.16)$$

$$\mu = 448.9 \times 10^{-6} \frac{\text{kg}}{\text{m s}}$$

$$c_p = \left[0.40188 + T_{film_K} \times (1.65007 \times 10^{-3} + 1.51494 \times 10^{-6} \times T_{film_K} - 6.67853 \times 10^{-10} \times T_{film_K}^2)\right] \times 10^3 \quad (B.17)$$

$$c_p = 959.03 \frac{\text{J}}{\text{kg K}}$$

$$\rho = 16.0184533 \times (36.32 + 61.146414 \times \psi^{\frac{1}{3}} + 16.418015 \times \psi + 17.476838 \times \psi^{\frac{1}{2}} + 1.119828 \times \psi^2) \quad (B.18)$$

where

$$\psi = 1 - \left(\frac{1.8 \times T_{film_K}}{753.95}\right) \quad (B.19)$$

$$\psi = 0.3407$$

and

$$\rho = 1520.96 \frac{\text{kg}}{\text{m}^3}$$

$$k = 0.071 - (0.000261 \times T_{film}) \quad (B.20)$$

$$k = 0.071 - (0.000261 \times 3.008)$$

$$k = 0.070215 \frac{W}{m K}$$

$$Pr = c_p \times \frac{\mu}{k} \quad (B.21)$$

$$Pr = 959.03 \times \frac{448.9 \times 10^{-6}}{0.070215}$$

$$Pr = 6.13$$

$$\beta = \frac{1}{\rho} \times \frac{\rho_{2.908} - \rho_{3.108}}{0.2} \quad (B.22)$$

where

$$\rho_{2.908} = 1521.24$$

$$\rho_{3.108} = 1520.68$$

then

$$\beta = \frac{1}{1520.96} \times \frac{1521.24 - 1520.68}{0.2}$$

$$\beta = 1.831 \times 10^{-3} \frac{1}{K}$$

$$v = \frac{\mu}{\rho} \quad (B.23)$$

$$v = \frac{448.9 \times 10^{-6}}{1520.96}$$

$$v = 295.14 \times 10^{-9} \frac{m^2}{s}$$

$$\alpha = \frac{k}{\rho \times c_p} \quad (B.24)$$

$$\alpha = \frac{0.070215}{1520.96 \times 959.03}$$

$$\alpha = 48.14 \times 10^{-9} \frac{m^2}{s}$$

Using the above calculated physical properties, h_b is obtained by iteration

$$h_b = 155.58 \frac{W}{m^2 K}$$

and

$$q_f = (h_b \times p \times k_{cu} \times A_c)^{0.5} \times \Delta T \times \tanh(n \times L_c)$$

becomes

$$q_f = (155.58 \times 49.64 \times 10^{-3} \times 402.95 \times 90.38 \times 10^{-6})^{0.5} \\ \times 1.48 \times \tanh \left[\left(\frac{155.58 \times 49.64 \times 10^{-3}}{402.95 \times 90.38 \times 10^{-6}} \right)^{0.5} \times 0.0264 \right]$$

$$q_f = 0.2877 W$$

The corresponding result for the three inch long end is obtained as

$$h_b = 134.37 \frac{W}{m^2 K}$$

$$q_f = 0.569 W$$

The heat transferred from heated portion is calculated as follows

$$q = 283.58 - 0.569 - 0.2877 \quad (B.25)$$

$$q = 282.72 \text{ W}$$

Then the heat flux and heat transfer coefficients are obtained from

$$q'' = \frac{q}{A_s} \quad (B.26)$$

$$q'' = \frac{282.72}{\pi \times D_o \times L}$$

$$q'' = \frac{282.72}{\pi \times 0.0158 \times 0.2032}$$

$$q'' = 2.8 \times 10^4 \frac{\text{W}}{\text{m}^2}$$

$$h = \frac{q''}{\Delta T} \quad (B.27)$$

$$h = \frac{282.72 \times 10^4}{1.48}$$

$$h = 1.89 \times 10^4 \frac{\text{W}}{\text{m}^2 \text{ K}}$$

APPENDIX C. UNCERTAINTY ANALYSIS

A method to predict the uncertainty of single sample measurements was suggested by Kline and McClintock [Ref 22] using a second order equation. If

$$R = R(x_1, x_2, \dots, x_n) \quad (C.1)$$

then the uncertainty in R, (δR), is given as follows

$$\delta R = \left[\left(\frac{\partial R}{\partial x_1} \delta x_1 \right)^2 + \left(\frac{\partial R}{\partial x_2} \delta x_2 \right)^2 + \dots + \left(\frac{\partial R}{\partial x_n} \delta x_n \right)^2 \right]^{\frac{1}{2}} \quad (C.2)$$

where, $\delta x_1, \delta x_2, \dots, \delta x_n$ are uncertainties in the n variables. The heat transfer coefficient is given by

$$h = \frac{q}{A_s \times (\bar{T}_{wo} - T_{sat})} \quad (C.3)$$

The outer average wall temperature (\bar{T}_{wo}) was obtained from following equation where \bar{T}_{wi} shows the average inner wall temperature which was measured by the wall thermocouples.

$$\bar{T}_{wo} = \bar{T}_{wi} - \frac{q \times \ln\left(\frac{D_o}{D_i}\right)}{2 \times \pi \times k_{cu} \times L} \quad (C.4)$$

In equation C.4, the second term on the right is called the Fourier conduction term. Let us define this term as

$$\Phi = \frac{q \times \ln\left(\frac{D_o}{D_i}\right)}{2 \times \pi \times k_{cu} \times L} \quad (C.5)$$

and

$$\Delta T = \bar{T}_{wo} - T_{sat} \quad (C.6)$$

The uncertainty in the heat transfer coefficient is obtained from the following equation

$$\frac{\delta h}{h} = \left[\left(\frac{\delta q}{q} \right)^2 + \left(\frac{\delta A_s}{A_s} \right)^2 + \left(\frac{\delta \bar{T}_{wt}}{\Delta T} \right)^2 + \left(\frac{\delta \Phi}{\Delta T} \right)^2 + \left(\frac{\delta T_{sat}}{\Delta T} \right)^2 \right]^{\frac{1}{2}} \quad (C.7)$$

where

$$q = V \times I \quad (C.8)$$

$$\frac{\delta q}{q} = \left[\left(\frac{\delta V}{V} \right)^2 + \left(\frac{\delta I}{I} \right)^2 \right]^{\frac{1}{2}} \quad (C.9)$$

where $\frac{\delta V}{V}$ and $\frac{\delta I}{I}$ are given accuracy of sensors which were used in experimentation. Calculation of surface area and the uncertainty of it were given as

$$A_s = \pi \times D_o \times L \quad (C.10)$$

$$\frac{\delta A_s}{A_s} = \left[\left(\frac{\delta D_o}{D_o} \right)^2 + \left(\frac{\delta L}{L} \right)^2 \right]^{\frac{1}{2}} \quad (C.11)$$

$\frac{\delta D_o}{D_o}$ and $\frac{\delta L}{L}$ are estimated quantities.² The uncertainty calculation of the Fourier conduction term is given below.

$$\frac{\delta \Phi}{\Phi} = \left[\left(\frac{\delta q}{q} \right)^2 + \left(\frac{\delta k_{cu}}{k_{cu}} \right)^2 + \left(\frac{\delta L}{L} \right)^2 \right]^{\frac{1}{2}} \quad (C.12)$$

k_{cu} was calculated using below equation

$$k_{cu} = 434.0 - (0.112 \times \bar{T}_{wi-K}) \quad (C.13)$$

so uncertainty in k_{cu} can be found as

$$\delta k_{cu} = [(0.112 \times \delta \bar{T}_{wi-K})^2]^{\frac{1}{2}} \quad (C.14)$$

² Work-shop device and human error in length and diameter measurements.

$\delta \bar{T}_{wi}$ and δT_{sat} were obtained using uncertainties in the thermocouple readings.³ The average wall inside temperature \bar{T}_{wi} was obtained by taking average of six wall thermocouple readings. The uncertainty in this temperature was calculated as

$$\delta \bar{T}_{wi} = \left[6 \times \left(\frac{\delta TC}{6} \right)^2 \right]^{\frac{1}{2}} \quad (C.15)$$

and saturation temperature was obtained from average of two liquid thermocouples reading and uncertainty in this temperature was calculated from following equation.⁴

$$\delta T_{sat} = \left[2 \times \left(\frac{\delta TC}{2} \right)^2 \right]^{\frac{1}{2}} \quad (C.16)$$

Using the above explanation, an uncertainty analysis was performed. File "FIND01" was used as the data source for the analysis. The high heat flux level was chosen to be 9.43 kW/m² and the low heat flux level was 1.69 kW/m² for the tabulated results in Table 9.

³ The uncertainty in type-T copper-constantan thermocouple reading δTC was obtained as ± 0.5 C from "Omega 1987 Complete Temperature Measurements Handbook pp. T-37".

⁴ Since the saturation temperature was very low, $\frac{\delta T_{sat}}{T_{sat}}$ created quite big percentage.

Table 9. UNCERTAINTY ANALYSIS RESULTS

Variable	High Heat Flux	Low Heat Flux
ΔT	7.41	2.06
\bar{T}_{wi}	10.00	4.34
T_{sat}	2.17	2.22
$\frac{\delta V}{V}$	0.005	0.005
$\frac{\delta I}{I}$	0.005	0.005
$\frac{\delta q}{q}$	0.0071	0.0071
$\frac{\delta D_o}{D_o}$	0.001	0.001
$\frac{\delta L}{L}$	0.001	0.001
$\frac{\delta A_s}{A_s}$	0.0014	0.0014
$\frac{\delta \bar{T}_{wi}}{\bar{T}_{wi}}$	0.0204	0.047
$\frac{\delta T_{sat}}{T_{sat}}$	0.163	0.159
$\frac{\delta k_{cu}}{k_{cu}}$	0.00034	0.00034
$\frac{\delta \Phi}{\Phi}$	0.0072	0.0072
$\frac{\delta h}{h}$	0.056	0.20

LIST OF REFERENCES

1. Nishikawa, K. and Ito, T. *Augmentation of Nucleate Boiling Heat Transfer by Prepared Surfaces*, Japan-United States Heat Transfer Joint Seminar, Tokyo, September, 1980.
2. Wanniarachchi, A.S., Marto, P.J. and Reilly, J.T. *The Effect of Oil Contamination on The Nucleate Pool-Boiling Performance of R-114 from a Prous-Coated Surface*, ASHRAE Transactions, vol. 92, Part 2, 1986.
3. Anderson, C.L., *Nucleate Pool Boiling Performance of Smooth and Finned Tube Bundles in R-113 and R-114/Oil Mixtures*, Master's Thesis, Naval Postgraduate School, Monterey, California, June, 1989.
4. Chongrungreong S., Sauer H. J., *Nucleate Boiling Performance of Refrigerants and Refrigerant-Oil Mixtures*, Journal of Heat Transfer, Vol. 102, pp. 701-705, November 1980.
5. Fujita Y., Ohta H., Hidaka S., Nishikawa K., *Nucleate Boiling Heat Transfer on Horizontal Tubes in Bundles*, Proc. 8th IHTC, San Francisco (1986), pp. 2131-2136.
6. Mikic, B. B. and Rohsenow, W. M., *A New Correlation of Pool-boiling Data Including the Effect of Heating Surface Characteristics*. Journal of Heat Transfer 91 (1969), pp. 245-250.
7. Chen Q., Windisch R., Hahne E., *Pool Boiling Heat Transfer on Finned Tubes*. Eurotherm No.8, Advances in Pool Boiling Heat Transfer, Paderborn FRG, May 11-12 1989.
8. Danilova, G. N., Dyundin, V. A., *Heat Transfer with Freons 12 and 22 Boiling at Bundles of Finned Tubes*. Heat Transfer Soviet Research, Vol. 4, No. 4, July-August 1972.

9. Sauer, H. J., Davidson, G. W., Chongrungreong, S., *Nucleate Boiling of Refrigerant-Oil Mixtures from Finned Tubing*, National Heat Transfer Conference, Orlando, Florida, July 27-30, 1980.
10. Yilmaz, S. and Palen, J. W., *Performance of Finned Tube Reboilers in Hydrocarbon Service*, ASME Paper NO. 84-HT-91, 1981.
11. Hahne, E. and Muller, J., *Boiling on a Finned Tube and a Finned Tube Bundle*; Int. J. Heat Mass Transfer. Vol, 26, No. 6, pp. 849-859, 1983.
12. Yilmaz, S., Hwalek, J. J. and Westwater, J. W., *Pool Boiling Heat Transfer Performance for Commercial Enhanced Tube Surfaces*, ASME paper No.80-HT-41, Orlando, July 1980.
13. Marto, P. J. and Lepere, V. J., *Pool Boiling Heat Transfer from Enhanced Surfaces to Dielectric fluids*, Journal of Heat Transfer, Vol. 104 (May) pp. 292-299.
14. Sawyer, L. M., Jr., *The Effects of Oil Contamination on the Nucleate Pool-Boiling Behavior of R-114 from Enhanced Surfaces*, Master's Thesis, Naval Postgraduate School, Monterey, California, December, 1986.
15. Grant, I., Hewitt, G., F. and Qureshi, J., *Pool Boiling of R-113/Oil mixtures on a High Flux Tube* Euroterm No. 8, Advances in Pool Boiling Heat Transfer, Paderborn, FRG, May 11-12, 1989, pp. 169-172.
16. Murphy, T.J., *Pool Boiling of R-114/Oil Mixtures from Single Tube and Tube Bundles*, Master's Thesis, Naval Post Graduate School, Monterey, California, September 1987.
17. Freon Product Information, "freon" Fluorocarbon Properties and Applications, by Dupont, p. 4, 1975.
18. Reilly, J. T., *The Influence of Oil contamination on Nucleate Pool Boiling Behaviour R-114 from a Structured Surface*, Master's Thesis, Naval Postgraduate School, Monterey, California, March 1985.

19. Fujita, Y., Ohta, H., Yoshida, K., Hidaka, S., and Nishikawa, K., *Nucleate Boiling Heat Transfer in Horizontal Tube Bundles (1st Report; Experimental Investigation on Tube Bundle Effect)*, Memoirs of the Faculty of Engineering, Kyusu University, Vol. 44, No. 4, pp. 427-446, 1984.
20. Churchill, S. W., Chu, F. H. S., *Correlating Relations for Laminar and Turbulent Free Convection from a Horizontal Cylinder*, International Journal Heat Mass Transfer, Vol. 18, pp. 1049-1070, 1975.
21. Pulido, R. J., *Nucleate Pool Boiling Characteristics of Gewa-T Finned Surfaces in Freon-113*, Master's Thesis, Naval Postgraduate School, Monterey, California, September 1984.
22. Kline, S. J., McClintock, F. A., *Describing Uncertainties in Single Sample Experiments*, Mechanical Engineering, p. 3, 1953.

INITIAL DISTRIBUTION LIST

		No. Copies
1.	Defense Technical Information Center Cameron Station Alexandria, VA 22304-6145	2
2.	Library, Code 0142 Naval Postgraduate School Monterey, CA 93943-5002	2
3.	Department Chairman, Code 69 Department of Mechanical Engineering Naval Postgraduate School Monterey, CA 93943-5000	1
4.	Professor Paul J. Marto, Code 69Mx Department of Mechanical Engineering Naval Postgraduate School Monterey, CA 93943-5000	5
5.	Mr. R. Helmick, Code 2722 David Taylor Research Center Annapolis, Maryland 21402-5067	1
6.	Mr. J. Hanrahan, Code 2722 David Taylor Research Center Annapolis, Maryland 21402-5067	1
7.	Mr. A. Smookler NAVSEA (Code 05R32) Department of the Navy Washington, D.C. 20362-5101	1
8.	Dr. J. DeCorpo NAVSEA (Code 56YB) Department of the Navy Washington, D.C. 20362-5101	1
9.	Mr. Bruce G. Unkel NAVSEA (Code 56Y15) Department of the Navy Washington, D.C. 20362-5101	1
10.	Dz. Kd. Utgm. Nezih Akcasayar Cinar Mah. 34. sokak No : 9 Camdibi Izmir / TURKEY	3

- | | | |
|-----|--|---|
| 11. | Deniz Kuvvetleri Komutanligi
Personel Daire Baskanligi
Bakanliklar-Ankara / TURKEY | 1 |
| 12. | Deniz Harp Okulu Komutanligi
Tuzla - Istanbul / TURKEY | 2 |
| 13. | Ortadogu Teknik Universitesi
Makina Muh.
Ankara / TURKEY | 1 |
| 14. | Istanbul Teknik Universitesi
Makina Muh.
Istanbul / TURKEY | 1 |
| 15. | Dokuz Eylul Universitesi
Makina Muh.
Izmir / TURKEY | 1 |